SUMMERTIME OZONE BEHAVIOR ALONG A VERTICAL TRANSECT NEAR THE DENVER, COLORADO METROPOLITAN AREA

A THESIS

Presented to

The Faculty of the Environmental Studies Program

The Colorado College

In Partial Fulfillment of the Requirements for the Degree

Bachelor of Arts in Environmental Science

By

Tiantian Zhu

May 2022

_____

Dr. Lynne Gratz

Associate Professor of Environmental Science

_____

Dr. Howard Drossman

Professor, Chair of Education Department

Acknowledgement

I would like to thank Dr. Lynne Gratz, my advisor and thesis mentor, for encouraging me and guiding me through this two-year-long project. Funding for this project was provided by the Colorado College Student-Faculty Collaborative Research (SCoRe) Program. I would also like to thank Erick Mattson from Air Pollution Control Division of Colorado Department of Public Health and Environment for providing this interesting dataset for me to explore and see how scientific analysis can inform regulatory changes. I am also grateful for Matt Cooney, the GIS Technical Director at Colorado College, for the support on GIS mapping and Brandon Chan for the help on HYSPLIT data retrieval. Thanks also to Dr. Howard Drossman for offering detailed feedback as the second thesis reader.

Abstract

Denver, Colorado in the Northern Front Range of the Rocky Mountains is a nonattainment area for ground-level ozone. In addition to local precursor emissions such as heavy motor vehicle usage and an active oil and natural gas industry, summertime ozone levels in this area are further influenced by western U.S. wildfires as well as complex flow patterns related to the elevated terrain and diurnal mountain-valley winds. Numerous studies have investigated air quality in the Denver basin, and the persistent high levels of summertime ozone emphasize the ongoing need for monitoring and mitigation for the protection of public health. In summer 2017, the Colorado Department of Public Health & Environment measured hourly ozone at seven sites along a vertical transect on the eastern slope of the Rocky Mountains, from Golden, CO (1839m ASL, 39.743°N, 105.179°W) to Mines Peak (3683m ASL, 39.794°N, 105.764°W) to determine the vertical extent and temporal variability of the Denver ozone plume. Hourly temperature, wind speed and direction were measured at five of the sites. Mean ozone increased by 1.0 ppb per 100m for the four lowest elevation sites (up to Black Hawk, 2627m ASL), which is a smaller slope than was determined in a previous vertical transect in the Northern Front Range as well as in vertical gradients at more rural mountainous sites. At these same four sites, diurnal amplitudes in hourly mean ozone generally decreased with increasing elevation, from 26 ppb to 13 ppb, and the effects of katabatic mountain wind patterns on diurnal ozone levels were evident. In contrast, two higher elevation sites, Jim Creek (3104 m ASL) and St Mary (3163 m ASL), showed weaker associations with katabatic wind patterns, significantly lower mean ozone concentrations than adjacent lower elevation sites, and larger ranges in hourly concentrations across the sampling period. However, Jim Creek was also situated in a different airshed and on the upwind side of Continental Divide so as to examine possible spill-over of Denver air masses, which occurred infrequently but resulted in elevated ozone levels when it did. Mines Peak appeared to serve as a regional background site, with little influence from daytime photochemical production or nighttime depositional losses. An identified regional fire event in early September 2017, resulting in a high ozone episode, was assessed using a combination of local criteria pollutant measurements, satellite imagery, and air mass back-trajectories.

1. Introduction

Tropospheric ozone is a secondary air pollutant formed by photochemical reactions of nitrogen oxides (NO_x) in the presence of carbon monoxide (CO), methane (CH_4), and volatile organic compounds (VOCs) (Jaffe et al., 2018). These precursors of ozone can be emitted from fossil fuel combustion, oil and gas production, biomass burning, motor vehicle exhaust, industrial facilities, and electric utilities (US EPA a). Breweries and marijuana grow houses also began to be recognized as major VOC contributors (Oldham, 2020; State of Colorado). Exposure to ozone is found to be associated with adverse health effects, such as asthma and premature death, and ecosystems damage, such as physiological injury of vegetation and decline in crop yields (Musselman et al., 2006; Felzer et al., 2007; McDonald-Buller et al., 2011 and references therein). In addition to being produced by photochemical reactions involving local precursor emissions, ozone is the only one among the six criteria pollutants regulated by the U.S. Clean Air Act that has a significant portion of background concentrations that remain beyond local control (Langford et al., 2017; Jaffe et al., 2018). U.S. background ozone refers to ozone formed from natural precursors and anthropogenic precursors from countries outside the U.S., and in some locations can make it challenging to quantify and regulate locally produced ozone (Jaffe et al., 2018). Compared to other criteria pollutants, surface ozone also shows more spatially and temporally variable trends in response to mitigation strategies (Austin et al., 2015). For example, peak ozone concentrations have the largest decrease in the eastern United States and in California, while most high-elevation and rural monitoring sites display either smaller declines or no significant change (Jaffe et al., 2018).

After periodic review of air quality criteria over the past few decades, in 2008 the U.S. Environmental Protection Agency (EPA) lowered the Primary and Secondary National Ambient Air Quality Standards (NAAQS) from 0.08 ppm to 0.075 ppm (75 ppb) for ozone concentrations (US EPA b). In 2015, the NAAQS was reduced to 70 ppb and a future revision may be between 60 to 70 ppb (US EPA, 2010; McDonald-Buller et al., 2011; Fine et al., 2015). Compliance with this standard is based on the 3-year average of the annual 4th highest maximum daily 8-h average (MDA8). The tightened standards further add urgency to the need for better interpreting surface ozone behavior and its drivers in different environments (Cooper et al., 2015). In the Western U.S., a great portion of the population resides in regions that exceed the NAAQS for ozone even before the standard was strengthened in 2015 (Cooper et al., 2011). Studies have

indicated local air pollution and long-range transport, often impacted by stratospheric intrusions and trans-Pacific pollution plumes, both contribute to enhanced local ozone. Yet local sources are often known to be a stronger driver of ozone standard exceedances mainly in urbanized areas of Western U.S. (Cooper et al., 2011 and references therein).

The Colorado Northern Front Range Metropolitan Area (NFRMA) is a non-attainment area for ozone with increasing or leveling-off trends over past decades (Strode et al., 2015; Flocke et al., 2019; Pfister et al., 2019; CDPHE, 2021; Crooks et al., 2021). The NFRMA encompasses the city of Denver, Boulder, Longmont, Ft. Collins, and Greeley, in which the urban areas and population are rapidly growing (Oltmans et al., 2019). This metropolitan area is home to almost three million people and is among the nation's fastest-growing urban centers with a 50% increase in population expected by 2030 (MetroDenver, n.d.). To the east of this region are major oil and gas developments and fast growing agricultural and livestock industries, leading to large emissions of ozone precursors (Abeleira et al., 2017; Oltmans et al., 2019). In summertime, this region tends to repeatedly experience high ozone episodes and is considered as an ozone non-attainment area by EPA (Abeleira et al., 2017; Cooper et al., 2014; Simon et al., 2015). Numerous studies have suggested the challenges of examining and forecasting the ozone behavior in this region due to the complex meteorology, varied terrain, and a mix of pollution sources involving local anthropogenic emissions, biogenic emissions, and wildfires (Flocke et al., 2019 and references therein).

To the west of the NFRMA, a set of 3000 m peaks rise abruptly and create dynamic geographical and meteorological regimes (Losleben et al., 2000). Meteorological conditions in this mountain-valley region, with prevailing daytime upslope wind and nighttime downslope wind, are coupled with daytime photochemical production and nighttime loss (Oltman et al., 2019). This regime on a local scale has been found to be related to elevated ozone occurrences (Toth and Johnson, 1985; Pfister et al., 2017; Evans and Helmig, 2016). As described in many previous studies, when the sun rises, the top valley walls are warmed first, driving the upslope anabatic winds, typically occurring during daytime in calm sunny weather, from the valley floor (Losleben et al., 2000; Mattson and Stauffer, 2016). While this happens, urban precursor emissions emerge, mainly related to morning rush hour traffic and industrial activities, and get carried up in anabatic winds. As the sun angle increases from morning to afternoon,

photochemical activity increases and drives ozone production as upslope flows continue to transport valley air up to elevated regions. As the sun angle decreases in the late afternoon, the canyon walls cool and surrounding air becomes denser and sinks creating downslope katabatic winds. Because certain anthropogenic emissions may continue in the absence of sunlight after sunset, nitric oxide can react with in-situ surface ozone or ozone that is blown down from higher elevations, acting as a chemical loss process for ozone (Mattson and Stauffer, 2016). This titration effect combined with surface deposition causes ozone mixing ratios to decline near the lower-elevation urban area during nighttime (Puxbaum et al., 1991; Jaffe et al., 2018; Bien and Helmig, 2018).

Boundary layer entrainment has been demonstrated by models and observational studies as an additional important driver of surface ozone in high elevation regions (Lehning et al., 1998; Aneja et al., 2000; Trousdell et al., 2016; Caputi et al., 2019). After sunset, due to the decrease of the convective thermals and radiative cooling, the stable nocturnal inversion layer forms (Stull, 1988; Hu et al. 2018). The pollutants and trace gases, including ozone, from the emissions and photochemical production at the top portion of the daytime mixed layer can remain in the residual layer overlying the nocturnal boundary layer (Hu et al., 2018). The convective thermals in the morning drive boundary layer growth and the entrainment of the residual layer ozone (Trousdell et al. 2016, Caputi et al. 2019). The downward-mixed residual air primarily consists of regional transport and local photochemical production of ozone from the previous day (Aneja et al., 2000 and references therein). Kaser et al. (2017) discovered this entrainment effect was the most important factor in the early morning among six surface sites in NFRMA, while local chemical production dominates later in the day.

Considering the topography, population density, and mixture of precursor emission sources, the vertical distribution of ozone in the Denver basin may be influenced by a combination of meteorological and chemical variables (Pfister et al., 2019). Understanding how ozone varies with elevation can help address the concerns for human health and vegetation (Brodin et al., 2010). Previous ozone-monitoring studies have found the background tropospheric gradient of increasing ozone concentrations with increasing elevation, but the magnitude of this gradient varies with seasons, geographical regions, and types of environments (urban or remote) (Brodin et al., 2010; Flynn et al., 2021 and references therein). Summertime ozone has been a

particular public health challenge because high insolation, frequent presence of high-pressure zones, and low wind speed can be conducive to the formation and accumulation of surface ozone (Mueller, 1994). Besides the synoptic conditions, previous studies have also indicated the major roles of the aforementioned thermally driven, terrain-induced diurnal flow patterns in NFRMA during summer (Flocke et al., 2019 and references therein). A better understanding of the ozone behavior during this period may allow regulatory agencies to optimize monitoring networks and identify where public health and ecological systems might be at risk (Cooper and Peterson, 1999).

In this work, we will characterize the vertical extent of the Denver ozone plume and the accompanying meteorological and topographical features through an analysis of measurements taken along a transect of seven sites from Golden, CO (NREL; 1839m ASL) to Mines Peak (3683m ASL). Section 2 provides an overview of the measurement stations and the statistical approaches used for examining ozone behavior both locally at each station and across the vertical transect. Section 3.1 examines ozone's statistical overview, diurnal variations, and regional influences at the seven sites, while Section 3.2 discusses the ozone vertical gradient and its variation on diurnal and seasonal time scales. Section 3.3 provides a case study analysis for a prolonged regional fire event in early September 2017. This study aims to add to the body of literature about the spatial and temporal behavior of ground-level ozone in the NFRMA.

2. Methods

2.1 Site locations and measurement methodologies

In 2017, in addition to two long-term permanent ozone monitoring sites in Golden, CO (NREL; 1839m ASL; 1994-present) and Mines Peak (3683m ASL; 2014-present), the Colorado Department of Public Health and Environment (CDPHE) Air Pollution Control Division (APCD) deployed five temporary measurement sites along a vertical transect outside of the Denver Metropolitan Area (Table 1; Figure 1). From 1 June to 30 September 2017, hourly measurements of ozone were collected at all sites and wind speed, wind direction, and temperature were collected at the temporary sites, Centennial, Vernon, Black Hawk, Jim Creek, and St. Mary. The sites in this study were chosen by a team of CDPHE meteorologists, modelers, and air quality

scientists to capture the height and behavior of the ozone plume from the Denver Metropolitan Area. Jim Creek was excluded from the elevation profile in Figure 1 because it was situated on the other side of the Continental Divide and was thus likely in a different airshed. The goal of siting at Jim Creek was to investigate whether the Denver ozone plume that reached the Continental Divide would spill over into the Frasier Valley. Following this data collection in summer 2017, Black Hawk was added as a permanent site by CDPHE in July 2019. We thus obtained hourly ozone measurements at the three permanent sites from summer 2019 onward to explore how the ozone vertical gradient varied throughout seasons and years.

During the 2017 study period, hourly ozone mixing ratios at NREL and Mines Peak were measured using Teledyne API (TAPI) 400E ozone analyzers. The TAPI 400 has a detection limit of 0.4 ppb and a measurement precision greater than 0.5 ppb or 0.5% of the reading. Hourly data from permanent monitoring sites are available online through the U.S. EPA Air Quality System (AQS). Hourly ozone data at the five temporary sites were collected using 2B Technologies Model 205 ozone analyzers. The 2B Tech ozone analyzers have a 1-σ measurement precision that is greater than 1.0 ppb or 2% of the reading (2B Technologies, 2018). At all stations, sampling heights were 2 m above ground, and the 2B Tech analyzers were contained in weatherproof, temperature-controlled enclosures. The 2B Tech 205 analyzers had baseline testing at midnight for 10 minutes, which was only used to detect drift and did not result in any alteration or adjustment to the data. No significant drift was found on the analyzers during the study. Once per month the precision was also checked using a Model 306 ozone source, which was calibrated against a Level II NIST traceable ozone source that is calibrated once per year against the Level I ozone source at EPA Region 8. Adjustments made during monthly precision checks were all within established limits. No adjustments to data were made due to an adjustment to the instrument calibration; any data that did not past quality control (> ± 3ppb) criteria would be flagged as invalid. Meteorological data was collected at five of the seven sites using Weather Meters with wind vane and cup anemometer (Shenzhen Fine Offset Electronics Co., Ltd; https://cdn.sparkfun.com/assets/d/1/e/0/6/DS-15901-Weather_Meter.pdf).

2.2 Data processing and statistical analysis

Summary statistics, linear regression analysis, significance tests for ozone measurements among all sites, and the relationships between ozone and meteorological data were determined using a combination of R Studio Version 4.0.5 (2021-03-31) and Microsoft Excel Version 16.57 (22011057). The Open Air package (version: 12th November 2019) in R studio was also used to generate wind roses that present ozone mixing ratios as a function of wind speed and direction. Locations of point-source emissions for NO_x and VOCs in the Denver Metropolitan Area were obtained from the U.S. EPA 2017 National Emissions Inventory (EPA, 2021a) and plotted using ArcGIS Pro 2.8.6.

One-way ANOVA tests and Tukey Honest Significance Differences were used to test the statistical difference in hourly ozone levels among sites. Statistical significance is reported at p-values < 0.05. For all diurnal analyses, daytime was regarded as the period from 6:00 to 19:00 MST and nighttime as from 20:00 to 5:00 MST. Instead of using the conventional two 12-hour periods, we chose the daytime and nighttime periods based on the typical sunrise and sunset times during summer in Colorado. For comparison of diurnal trends, studies referenced could be based on different sets of daytime and nighttime hours.

2.3 Regional wildfire case study

The September 4-6 event was chosen for case analysis because of the previously identified fire complex in the western U.S. To confirm the impact from wildfire, we retrieved the NOAA Hazard Mapping System (HMS) Fire and Smoke Product (AirNow Tech, 2021) to determine the presence of overhead smoke. We also used daily $PM_{2.5}$ data from the CDPHE permanent air monitoring site at Chatfield State Park to confirm the presence of ground-level smoke (EPA, 2021b). We first calculated the mean and standard deviation of $PM_{2.5}$ data during the periods without overhead smoke, as determined from the HMS product. Then, to identify days with ground-level smoke, we looked for days when $PM_{2.5}$ was greater than this non-smoke-day mean plus one standard deviation (> 9.7 $\mu g/m^3$) (Flynn et al., 2021). This September 4-6 period was found to have both overhead and higher, longer ground-level smoke, which reflect the length of the period of interest. We are looking to determine whether this prolonged regional fire event resulted in elevated ozone through comparing the mixing ratios within and outside of this period at 1000m AGL from the archive of NOAA Air Resources Laboratory (NOAA, 2022).

3. Results and Discussion

3.1 Data overview and site characterization

3.1.1 Ozone statistical behavior

The median hourly ozone mixing ratios were the highest at Centennial (54 ppb) and Black Hawk (55 ppb) and lowest at NREL (47 ppb). The range of measurements was greatest at Jim Creek (117 ppb) and smallest at Mines (54 ppb), which also had the smallest variability with a standard deviation of the mean of 8 ppb (Table 2). The medians increased with increasing elevation among the four lowest elevation sites, from NREL to Black Hawk, dropped at Jim Creek (49 ppb), and then increased from St Mary (49 ppb) to Mines Peak (52 ppb) (Figure 2). In addition to increasing median levels, the four lower elevation sites, from NREL to Black Hawk, showed decreasing variability around the mean as standard deviations decreased from 15 ppb to 11 ppb (Table 2). According to single factor one-way ANOVA tests, all sites' mean ozone measurements were statistically different from one another ($p<<0.0001$). For pair-wise comparisons of sample means, Tukey Honest Significant Differences reflected that only the differences between Centennial and Black Hawk (p-adj = 0.88), between NREL and Jim Creek (p-adj = 0.92), and between NREL and Mines Peak (p-adj = 0.75) were not statistically significant. Given that Jim Creek was located on the other side of the Continental Divide, and therefore was likely in a different airshed, it is perhaps not surprising that its median ozone did not fall along a linear vertical gradient with the other sites, and we will further investigate its distinct ozone behavior in following sections.

Hourly ozone concentrations at all seven sites are shown in a cumulative frequency plot in Figure 3, which allows for more directly comparing specific percentiles and contextualizing results with related studies, such as the work by Brodin et al. (2010) about a vertical transect outside of Boulder, CO in 2007 with comparable site elevations and mountainous topography. In this Denver study, all sites' cumulative frequency curves appeared linear, suggestive of Gaussian behavior of the middle concentration range of ozone at all sites (Brodin et al., 2010). One exception is that St. Mary had a convex curve below the 50^{th} percentile, deviating from a linear slope (Figure 3). There also was a difference of over 2 ppb between St. Mary's mean and median, while at the remaining sites the differences were below 1 ppb (Table 2). Because all differences were within the range considered by Brodin et al. (2010) as the indication of

Gaussian behavior, and the skewness of all sites was close to 0 (Table 2), we interchangeably use mean and median to compare the sites' overall ozone behavior in the subsequent discussion. In this 2017 Denver study, the cumulative frequency curves were relatively closely clustered, with a median difference between the seven sites of 8 ppb, compared to the median difference of about 25 ppb at sites in the Brodin et al. (2010) study. Despite the comparable elevation range and the same geographical region in Brodin et al. (2010)'s study, the highest site, Tundra lab, sometimes behaving as a background site, and the urban site, Central Boulder, had notably higher and lower medians than the rest of the sites, increasing the median range and the distance between cumulative frequency curves. This was driven by the Tundra Lab receiving the least amount ozone destruction and the urban site in Boulder experiencing the heavy traffic that suppressed ozone accumulation (Brodin et al., 2010).

Among all sites' cumulative frequency curves, the ones for the four lower elevation sites, from NREL to Black Hawk, were more closely clustered with each other, which is possibly related to similar transport and meteorological conditions influencing all four sites, thus a well-mixed boundary layer (Brodin et al. 2010). Jim Creek displayed lower slopes at the upper percentiles (> 95^{th} percentile), indicative of a strong influence of high-ozone event(s) (Brodin et al., 2010), which will be elaborated further in section 3.1.3. More extreme values shown on the higher end of the distribution were also apparent in Jim Creek's boxplot distribution (Figure 2 and Figure 3). St. Mary had a greater number of ozone measurements distributed at lower ozone mixing ratios (<50 ppb), as evidenced by its non-normal distribution and indicative of longer time spent in a low-ozone environment (Brodin et al., 2010). Yet St. Mary displayed a similar slope at upper percentiles as lower sites, indicative that its higher ozone measurements were about similar levels as lower sites. Mines Peak, as the highest elevation site, had a notably steeper slope compared to the remaining six sites, representative of a smaller spread of data.

3.1.2 Diurnal ozone behavior at individual sites

Excluding Mines Peak, which will be discussed separately, the average diurnal curves reflect typical daily tropospheric ozone production and loss cycles. The daily maxima of hourly-averaged ozone ranged from 59 ppb at St. Mary to 66 ppb at Vernon, which occurred around 13:00 to 14:00 MST (Figure 4 and Table 3). The minima, ranging from 32 ppb at St. Mary to 49

ppb at Black Hawk, occurred around 5:00 to 6:00 MST, followed by quick morning increases, up to 13 ppb/h at St. Mary. After reaching the daytime peaks, ozone mixing ratios dropped quickly by 15%-40% until 21:00 and then slowly decreased to the lowest levels in the early morning (Figure 4 and Figure 5). The timing and magnitudes of early afternoon peak ozone at sites excluding Mines Peak were similar to measurements reported in Flynn et al. (2021) and Brodin et al. (2010) for sites at varying elevations in Colorado Springs, CO and Boulder, CO. The peak time also overlapped with Ribas and Penuela's (2006) results.

This mechanism of daytime increases and nighttime decreases in ozone mixing ratios reflected, in part, the fact that sunlight drives photochemical reactions to form ground-level ozone during the day, while during the night ozone is consumed through surface deposition and NO titration, as described previously (Fine et al., 2015; Wang et al., 2006). Many previous studies have reported that photochemical production is vital during the day, whereas there has been variation among regions in whether reaction with NO or dry deposition is more important as the key ozone loss process (Caputi et al., 2019 and references therein). Other processes have been found to account for diurnal ozone budgets at each individual site, such as horizontal advection, vertical mixing, boundary layer entrainment, as well as regional transport (Conley et al., 2011; Trousdell et al., 2016; Caputi et al., 2019).

The diurnal change in ozone mixing ratios was greatest at NREL (amplitude = 26 ppb) and decreased up to Black Hawk (amplitude = 13 ppb) (Table 3). The decreasing amplitudes of diurnal cycles with increasing elevation among the four lower sites aligned with other studies, which attributed this behavior to greater surface deposition at low elevations and a stronger NO titration effect derived from proximity to precursor sources (Puxbaum et al., 1991; Mueller, 1994; Brodin et al., 2010; Flynn et al., 2021). The greater deposition at lower elevation could be driven by nighttime inversions (Aneja et al., 2000; Ambrose et al., 2011) and the smaller air volume-surface ratio compared to that at elevated sites (Puxbaum et al., 1991). From NREL to Black Hawk, aside from the decreasing amplitudes, the overall diurnal rates of change in ozone, timing of the daytime increase and nighttime decrease, and timing for peak and minimum values were consistent (Figure 4 and Figure 5). These observations among the four lower sites suggest that the boundary layer within the urban air shed was sufficiently well-mixed such that ozone mixing ratios at the sites increased and decreased simultaneously (Brodin et al., 2010).

St. Mary, with the greatest diurnal ozone amplitude of 27 ppb, had the lowest nighttime ozone (32-36 ppb from 21:00 to 6:00 MST next day) but a daytime maximum similar to other sites (59 ppb) (Figure 4 and Table 3). Different from the more gradual change of ozone observed in other sites, the average diurnal ozone mixing ratios had the fastest morning increase (with the maximum rate as 13 ppb/h at 7:00 MST), reached a plateau until 16:00 MST, and decreased drastically from 16:00 to 21:00 MST (with the maximum rate as -9 ppb/h at 19:00 MST) (Figure 4 and Figure 5). With a similar shape of the diurnal hourly ozone trend, Jim Creek also, but to a lesser degree than St Mary, tended to exhibit a box-shaped trend that differentiate this site from the lower four sites (Figure 4). Their relatively abrupt morning increase and evening decrease in combination with relatively long periods of daily high ozone could be attributed to different mechanisms of ozone formation, smaller likelihood of experiencing ozone destruction compared to lower sites, and meteorological drivers such as boundary layer entrainment that can be more pronounced at higher elevations due to closer distance to the free troposphere (Mueller, 1994). Also, Puxbaum et al. (1991) suggested that high mountain sites (below 2500m ASL in their case) could undergo a mixture of air that consists of free tropospheric air, continental boundary layer air, and air masses from local valleys. Though this study's data cannot confirm the role of individual effects, we speculate that Jim Creek and St Mary, two elevated sites above 3000m, experienced a more complex set of drivers of ozone behavior. In addition, at Jim Creek and St. Mary, there was a tendency that the morning average rate of increase was greater than the afternoon decrease rate, which might suggest a potential build-up of ozone. Brodin et al. (2010) observed a pronounced net chemical gain of ozone in summer only at the vertical transect in Boulder, CO, which they hypothesized that pollutants were trapped near the surface under stronger temperature inversions.

Mines Peak, the highest elevation and most remote site, had the smallest diurnal amplitude of hourly ozone (4 ppb) in a reverse trend from the other sites, with increasing nighttime ozone (Figure 4 and Table 3). Mueller (1994) observed smaller diurnal behaviors during both daytime and nighttime at a remote site in Great Smoky Mountains National Park. Monks et al. (1999) and Brodin et al. (2010) also identified the cycle of midday ozone destruction and no daily ozone production for high elevation background sites. These analogs of diurnal trends of remote sites combined with the smaller spread and low data variability throughout the entire study period led to our speculation of Mines Peak as a likely background

site that perhaps was partially in contact with air above the boundary layer and less affected by daytime local production in the Denver Metropolitan Area or nighttime loss processes (Mueller, 1994; Bien and Helmig, 2018; Brodin et al., 2010). Interestingly, Tukey's test of means revealed a statistically insignificant difference between NREL and Mines Peak, demonstrating that the average ozone mixing ratio at Mines Peak's was comparable to that at the lowest elevation NREL site that was most influenced by local urban pollution (Figure 2). Therefore, despite the minimal fluctuation of measurements at Mines Peak, sites that may be in contact with the free troposphere can experience relatively high mixing ratios within the large high-altitude ozone reservoir that encounters little dry deposition and destruction reactions (Mueller, 1994).

Being a background site does not imply being above the mixed layer, but a free tropospheric site mainly receives inputs from long-range transport and stratosphere-troposphere exchange (Ambrose et al., 2011; Jaffe, 2011; Thompson, 2019). Mines Peak had a similar extent of average diurnal variation of ozone compared to the highest site Tundra Lab in Brodin et al. (2010) study (3528m ASL, diurnal amplitude = 5 ppb), which was identified as a purely background site only in fall and winter. While Tundra Lab's diurnal ozone trend sat almost entirely above those of the lower elevation sites and exhibited the highest daily maximum, the diurnal ozone trend at Mines Peak cut across those at lower sites in the present study. This is also consistent with the more clustered cumulative frequency curves in this Denver study, which may indicate a stronger association between Mines Peak and the remaining lower sites. Additional data are required to confirm whether and when Mines Peak is situated within the free troposphere and if wind conditions can expose it to the mixed layer with the influence from the Denver Metropolitan Area. Water vapor may be a potentially helpful measurement as a marker of dry free tropospheric air and pollution tracers (Ambrose et al., 2011).

We also regressed the daytime ozone maximum against the previous night's average ozone. Though this technique was developed by Aneja et al. (2000) for a tower site to study the role of boundary layer entrainment, using this approach for surface sites can allow us to examine the role of nighttime loss processes at each site. We observed statistically significant correlations ($p < 0.01$) as well as Pearson R^2 values ranging from 0.06 at Black Hawk to 0.43 at Mines Peak (Table 4). In addition to the greatest correlation coefficient, Mines Peak had a slope close to 1, consistent with its relatively flat diurnal curve that actually contained no daytime maximum

(Figure 4). This therefore agrees with our hypothesis earlier in 3.1.2 that Mines Peak potentially acted as a background site that was relatively isolated from daytime production and nighttime destruction processes. Among the lower four sites, R^2 values and slopes decreased with increasing elevation (Table 4), suggestive of smaller influence of nighttime average ozone on next day's maximum at higher elevations. This could indicate a stronger influence of daytime transport at elevated sites.

3.1.3 Meteorological drivers of ozone: local wind and temperature

Meteorological drivers such as temperature, wind speed, and wind direction may influence ozone behavior along the vertical transect. A number of prior studies (e.g. Jaffe and Zhang, 2017 and references therein) have indicated that, under climate change, a better understanding of the association between these drivers and ozone production and accumulation is conducive to projecting future ozone trends and health impacts on different scales. From the regressions against hourly measurements of temperature and wind speed at Vernon, Centennial, Black Hawk, Jim Creek, and St. Mary, we observed statistically significant positive correlations at all sites ($p << 0.0001$) (Figure 6 and Figure 7). A strong relationship between hourly ozone and temperature is expected as sunlight drives photochemistry and thus plays a vital role in controlling local ozone production and loss, as discussed in 3.1.2. The regional katabatic winds that transport ozone up from urban precursor sources is thermally driven as well (Flynn et al., 2021; Camalier et al., 2007; Mattson and Stauffer, 2016).

Weaker but significant correlations (R^2 values ranging from 0.04 to 0.21) were found between ozone and wind speed (Figure 7). This is comparable to Flynn et al. (2021)'s finding and the conclusion that wind speed was not a particularly strong predictor of hourly ozone. Previous studies demonstrated that high wind speed could have two-way effects (Brönnimann et al., 2000). High wind can dilute ozone by aiding dispersion, and it also facilitates ozone buildup by transporting ozone and precursors up to rural, higher-elevation areas with weaker uptake processes (Brönnimann et al., 2000; Camalier et al., 2007; Jaffe and Zhang, 2017). Though St. Mary had a relatively strong linear correlation coefficient ($R^2 = 0.21$), its correlation appeared less linear compared to the other three sites and that some higher wind speeds were associated

with more moderate ozone (Figure 7). Vernon had the weakest correlation between hourly ozone and wind speed (R^2=0.04) and a clustered distribution.

In addition to wind speed, wind direction offers information about the effect of anabatic and katabatic mountain valley winds. As described previously, the morning anabatic winds can transport ozone and its precursors up in elevation, whereas the evening katabatic winds bring it down from elevated sites and facilitate the NO titration around the urban precursor sources (Mattson and Stauffer, 2016). At Centennial and Black Hawk, the day and night ozone wind roses exemplify this anabatic/katabatic wind pattern (Figure 8). At these two sites, the highest daytime ozone mixing ratios (6:00 to 19:00 MST) occurred under northeasterly flow, from the Denver Metropolitan Area, though Centennial also experienced some high ozone mixing ratios under southwesterly winds. During nighttime (20:00 to 5:00 MST), the highest ozone measurements generally occurred under southwesterly winds despite a few higher points associated with northeasterly flow (Figure 8). Interestingly, at Vernon, though higher ozone mixing ratios were observed with katabatic winds from the southwest, daytime higher ozone was mainly observed under southerly wind, not directly from the direction of the urban area. Thus, Vernon, as the site closest to urban precursors among the sites with wind measurements, did not entirely follow the diurnal valley wind patterns. Based on prior knowledge of the site, the higher ozone observed under southerly wind may reflect the transport of ozone under clockwise flow around high-pressure systems east of the Rocky Mountains that are frequently observed during summer months. Synoptic scale high-pressure systems were also believed as a contributor to high ozone mixing ratios in related studies (Mueller, 1994; Mattson and Stauffer, 2016). This combines with the weakest predicting power of local wind speed at Vernon (Figure 7) to imply a more synoptic-scale driver of the highest ozone events at Vernon, rather than local-scale meteorology. The stronger association of ozone at Centennial and Black Hawk with katabatic winds and with wind speed (Figure 7) is likely related to topography that is sloped towards the Denver Metro area and thus facilitates the transport of urban ozone (Flynn et al., 2021). Despite the possibly different effects of local topography and meteorology, the diurnal patterns of ozone displayed similar timing of the morning increase among the four lower sites. This suggests that the upslope wind transport and in-situ ozone formation happened almost synchronously (Figure 4

and Figure 5), consistent with the earlier claim that katabatic and anabatic advection resulted in a well-mixed boundary layer.

Compared to other sites' daytime wind speed, the wind roses at Jim Creek show lower wind speeds from all directions during the day (Figure 8). A few higher ozone mixing ratios were observed from the northeast and southwest during the day with some extreme values (over 70 ppb) observed under higher easterly winds. The nighttime wind rose at Jim Creek displays mainly northeasterly and easterly winds and higher ozone under easterly wind. Hence overall Jim Creek does not demonstrate the same diurnal wind pattern that lower elevation sites tended to experience, as it was intentionally placed on the other side of the Continental Divide and thus a different air shed (Figure 9a and b). The extreme ozone measurements under easterly flow in Jim Creek's daytime wind rose were taken during an identified fire event from September 4-6, as expanded in section 3.3. This event suggests that Jim Creek might either directly received higher concentration of ozone and its precursors or it might display the spillover effect that might only occurred a few times.

At St. Mary, the daytime wind rose shows predominantly northwesterly and southeasterly winds and generally lower ozone mixing ratios compared to other sites' daytime measurements, which aligns with the lower daytime average peak ozone at St. Mary (Figure 8 and Table 3). Some much lower daytime measurements (below 40 ppb) were seen under fast easterlies, which might be related to the NO titration effect owing to the I-70 highway (to the southeast) traffic during the day (Figure 9a and c). The generally lower daytime ozone mixing ratios at St Mary could also be potentially attributed to the proximity to the highway corridor. The nighttime higher ozone mixing ratios were observed under northwesterly winds. However, given the different diurnal ozone trend as well as the relationships between ozone and windspeed from the lower sites, one should not draw a conclusion that St. Mary followed the same trend of katabatic winds. We speculate that the highway corridor effect could act as a prolonged in-situ source for ozone formation during the day and a more direct and stronger source of ozone titration during the night (Figure 4). Because Vernon could also experience the highway corridor effect, additional data of temporal and spatial variability of precursor concentrations may help us better determine the highway's influence on ozone and meteorology at Vernon and St. Mary.

To explore ozone's dependence on temperature, we also regressed MDA8 ozone, the daily maximum value of the 8-h rolling average, at each site against daily maximum temperature. For example, Jaffe and Zhang (2017) and Flynn et al. (2021) found daytime maximum temperature to be a strong predictor of MDA8 ozone using linear regressions and Generalized Additive Models. All correlations were statistically significant ($p << 0.0001$) and had R^2 values ranging from 0.32 to 0.53 (Figure 10), comparable to the R^2 values found by Jaffe and Zhang (2017), ranging from 0.25 to 0.51, based on five-year data in multiple cities in the U.S. These strong correlations also align with results from many previous studies suggesting that temperature is one of the most important drivers in daily ozone mixing ratios (Camalier et al., 2007). This may be related to the fact that temperature likely covaries with other factors that aid ozone production and accumulation, involving air stagnation and solar insolation (Jaffe and Zhang 2017). To further look at the influence of temperature on ozone variability, $\Delta O_3/\Delta T$ of the regressions observed among our five sites ranged from 1.1-1.4 ppb/degree C (Figure 10), within the range of values (0.89 to 1.70 ppb/degree C) from the cities Jaffe and Zhang (2017) considered, but smaller than the range (1.8 to 2.2 ppb/degree C) found by Flynn et al. (2021) based on a six-year dataset in Colorado Spring. However, this $\Delta O_3/\Delta tT$ slope might vary with temperature range and the presence of smoke (Jaffe and Zhang, 2017; Steiner et al., 2010; Flynn et al., 2021). Steiner et al. (2010) found a decreased slope at the highest temperatures. Jaffe and Zhang (2017) also proposed that other drivers such as reduced wind speeds may counteract the effect of high temperatures.

To summarize the effects of these meteorological variables, wind speed acted as a relatively weak predictor of hourly ozone, and temperature was a stronger predictor of MDA8. Each site demonstrated distinct local wind direction influences. As a stronger predictor of ozone, the temperature impact on ozone can also be variable depending on the temperature range, wind speeds, and other meteorological factors. Instead of only looking at partial response, a detailed, long-term group analysis of meteorological factors, such as using the Generalized Additive Modeling (GAM), would be effective to explore the predictors for ozone (Camalier et al., 2007; Gong et al., 2017; Jaffe and Zhang, 2017; McClure and Jaffe, 2018; Flynn et al., 2021). Other than meteorological conditions, precursor measurements, including VOC and NO_x, may also indicate ozone variability (Jaffe and Zhang, 2017).

3.1.5 Regional ozone variability across the vertical transect

In addition to examining the localized drivers involving meteorology and terrain of ozone variability at each site along the vertical transect, we investigated the broader patterns in daytime ozone across the sites, especially during the mid-day peak period that is of greatest interest for the protection of public health. To do so, we conducted pair-wise Pearson correlations of MDA8 values among all sites (Figure 11). All regressions were statistically significant ($p << 0.001$) and R^2 values ranged from 0.14 to 0.91. The regressions all had positive slopes, implying some consistent variability in MDA8 ozone across the study sites; yet some differences were observed which help demonstrate the strength of these relationships across the transect.

The R^2 values were the smallest, ranging from 0.14 to 0.53, in the regressions against NREL for each of the other six sites (Figure 11), possibly indicating that, because NREL is closest to urban precursor sources, the heaviest exposure to local precursor emissions might suppress the ozone accumulation (Brodin et al., 2010). The weakest correlations (R^2=0.14 and 0.21) among all regressions were those between NREL and Mines Peak, and between NREL and Jim Creek. Interestingly, these weak correlations of highest ozone are not in alignment with the insignificant Tukey comparisons of means between these two groups. However, relatively strong MDA8 correlations between the three higher sites, St Mary, Jim Creek, and Mines Peak, (R^2=0.57 and 0.69) indicates the ozone concentration at those sites experienced relatively strong regional controls on daytime ozone.

Among all correlations the highest R^2 values (> 0.70) occurred between the other three lower elevation sites, Vernon, Centennial, and Black Hawk (Figure 11). The similar behavior of MDA8 ozone at these three sites suggests, again, that they were generally in the same well-mixed daytime pollution layer. St. Mary, as one of the high elevation sites above 3000m ASL, also had relatively strong correlations with these three sites (R^2 ranging from 0.66 to 0.69), inferring the influence of regional pollution from Denver Metropolitan Area on this site. The smaller intercepts (3.1 to 8.2 ppb) of the correlations between the three lower sites, Vernon, Centennial, and Black Hawk, also suggest smaller ozone accumulation over days and thus stronger effect of nighttime destruction. For each site, the correlation against Mines Peak has the greatest slopes, aligning with the previous statements in 3.1.2 that the background site

experiences the smallest influence of ozone loss processes, and it could likely be in contact with the ozone reservoir in the free troposphere.

3.2 Vertical ozone gradient and temporal variability

Average hourly ozone at the four lower elevation sites followed a strong linear correlation with increasing elevation, demonstrating that average ozone concentration increased by 1.0 ppb per 100 m (Figure 12b). In the northern Front Range of Colorado, along a vertical transect with a similar altitude range compared to the entire transect for this Denver study, Brodin et al. (2010) observed seasonal rates of ozone increase with elevation ranging from 1.1-1.7 ppbv per 100m based on one year of continuous measurements. Flynn et al. (2021) found a 2.0 ± 1.8 ppb per 100m increase in mean ozone based on surface measurements at eight sites in the Southern Front Range of the Rocky Mountains in summer 2018. Similar studies in remote mountainous regions of North America and Europe have reported vertical ozone gradients ranging from 1.2 to 3 ppb per 100m (Cooper and Peterson, 2000; Ribas and Penuelas, 2006; Chevalier et al., 2007; Flynn et al., 2021). The main driver of increasing ozone with elevation is found to be reduced surface deposition and longer ozone lifetime at higher elevation sites (Flynn et al. 2021 and citations therein; Chevalier et al. 2007). The decreasing error bar ranges, representing standard deviation, from NREL to Black Hawk also aligned with the trend of decreasing ozone variability with altitude found by Chavelier et al. (2007) (Figure 12) and is consistent with the more direct influence of boundary layer photochemistry at lower elevations that was described in 3.1.2. The slope of 1.0 ppb per 100 m determined in this study for Denver is a comparable but smaller positive gradient of ozone with elevation than that reported by all the aforementioned studies. This is due in part to the fact that we only included the four lower elevation sites because of the stronger ozone-altitude regression with these lower sites than that with all sites. This can be very different from the altitude range of other studies in which more remote regions may increase the tropospheric ozone gradient. Even for the lower range in altitude, the smaller slope could also imply relatively more well-mixed tropospheric air.

With the assumption that Jim Creek was located in another air shed, the vertical profile of ozone with the remaining six sites resembled a “bell shape” with an increasing ozone trend with

elevation at lower sites but decreasing trend at elevated sites (Figure 12a). This pattern was also found by Brodin et al. (2010) in their summer data, a summertime study by Bytnerowicz et al. (2002) at sites at elevations ranging from 500m to 2200m ASL, in Sequoia National Park, California, and a year-long study by Puxbaum (1991) conducted in an alpine valley at elevations from 600m to 2000m ASL. These studies together indicated that ozone dilution and deposition to vegetation exceeded the ozone formation potential from local precursors at higher sites, especially over 2000m ASL. Thus, the elevation range above the point where the "bell shape" bends down could be where the local formation or transport are outweighed by ozone loss processes.

Monthly average regressions of average ozone versus elevation also displayed high R^2 values (0.86 to 1.00) with slopes ranging from 0.6 to 1.2 ppb/100m (Figure 13). The steepest slope was reported in the month of September, perhaps indicating that with the seasonal transition to fall boundary layer mixing tends to become weaker (Brodin et al., 2011). These regressions, combined with earlier analyses, would seem to again verify that the summertime Denver ozone plume can be captured up to the elevation of Black Hawk (2627m ASL) as the highest site in this study. This can be supported by the diurnal trends that exhibit similar patterns among the four lower sites (Figure 4 & Figure 5), wind roses that show diurnal anabatic and katabatic winds at the Vernon, Centennial, and Black Hawk sites (Figure 8), and the pair-wise associations that demonstrate the similar response to MDA8 ozone influence among the lower sites (Figure 11). This finding therefore justifies the CDPHE's decision to add Black Hawk as a permanent site in summer 2019.

Knowing that ozone displayed a pronounced diurnal cycle at all sites except Mines Peak, we examined the average ozone mixing ratios at 12:00 MST and 1:00 MST for every site, as a representation of the vertical transects during periods of peak daytime and lowest nighttime ozone mixing ratios, respectively (Figure 14). Again, at the four lowest elevation sites we see overall increasing trends of ozone with increasing elevation both at midday and mid-night. However, the regression at noon showed a much weaker linear relationship between ozone and elevation (R^2=0.12) with a flatter slope (0.2 ppb per 100 m), while the midnight correlation showed a relatively strong linear regression (R^2 = 0.93) compared to the overall average gradient but a relatively steeper slope (1.4 ppb per 100 m) (Figure 12 and Figure 14). These separate

regressions reflect a more well-mixed daytime boundary layer, under which the four lowest elevation sites had more similar levels of ozone. This effective turbulent mixing process is consistent with the almost simultaneous increase among the lower sites as described in the diurnal trend and rates of daytime increase (Figure 4 and Figure 5). Yet during the night, the inversion layer and a more stratified boundary layer could lead to increasing effects of surface deposition and NO titration at lower elevation valley sites (Flynn et al., 2021). Excluding Jim Creek, that is likely in a different air shed, the mid-day average ozone at the remaining six sites displayed a generally decreasing trend with a slope of -0.6 ppb per 100 m (R^2=0.57) (Figure 14). Consistent with Aneja et al. (2000) and Ribas and Penuela (2004)'s observations of lower maximum ozone mixing ratio with increasing elevation based on multi-year data, this inverted mid-day ozone profile reflects the greater influence of daytime photochemical production of ozone at lower elevation sites (Chavelier et al., 2007).

Because the linear relationships between ozone and elevation were very strong at NREL, Vernon, Centennial, and Black Hawk (Figure 12 and Figure 13) and consistent month to month during the 2017 multi-site study, we elected to investigate the vertical gradient between just NREL and Black Hawk in subsequent seasons and years (when measurements were not simultaneously conducted at Vernon or Centennial), to comment on how the vertical ozone gradient may vary across years and seasons. In general, and as expected, colder seasons had lower average ozone mixing ratios because of the less active photochemistry (Figure 15). From summer 2019 to fall 2021, we calculated slopes ranging from 0.5 to 0.8 ppb per 100 m in spring, -0.6 to -0.4 ppb per 100 m in summer, 0.3 to 0.7 ppb per 100 m in fall, and 0.9 to 1.4 ppb per 100 m in winter (Figure 15). The net vertical gradient was greatest, or more positive, during winter among all seasons, which aligns with Brodin et al.'s observation of greater slopes in colder seasons and the calculated slope of 1.5 ppb 100 m during winter. This possibly related to a more stratified atmosphere with the lack of the thermally driven boundary layer mixing, which may lead to more similarity between Black Hawk and the free troposphere during winter (Brodin et al., 2010).

Brodin et al. (2010) also found that regional transport, rather than local production, acted as a predominant factor during fall through spring. Thus, with smaller local diurnal variation, the stagnation of pollutants may be more pronounced in these colder seasons, especially at higher

elevation sites. In addition, ozone deposition rates were believed to be higher during summer with stomatal uptake as the primary process, while non-vegetated deposition rates, such as on snow, were significantly lower (Wesely and Hicks, 2000). However, ozone enhancements over snow were also reported from various regions (Crawford et al., 2001; Helmig et al., 2008; Schnell et al., 2009). Therefore, with weaker loss processes in the snow-covered higher elevations, local photochemical activities, and a more stable, stagnant boundary layer, the growth in ozone mixing ratios with elevation would be expected to be larger in colder periods.

Ribas and Penuela (2006) found seasonal changes in maximum ozone mixing ratios at different elevations from measurements in May to December. They suggested that the valley-bottom sites had their maximum ozone concentrations in summer, while the upper-elevation sites have higher concentrations during cold periods, which was likely associated with the longer ozone lifetime with the lack of precursor emissions and non-photochemical sources such as the exchange between stratosphere and troposphere (Ribas and Penuela, 2006). This does not confirm the seasonal variations at NREL or Black Hawk themselves, but it could offer insights for interpreting the steeper vertical gradients in colder seasons.

Interestingly, after Black Hawk was added as a permanent site, all summers since 2019 displayed negative gradients between NREL and Black Hawk (-0.6 to -0.4 ppb per 100 m from 2019 to 2021). This contrasts with the positive gradient observed in summer 2017 (Figure 12). Drawing from Brodin et al. (2010)'s analysis of the "bell-shaped" vertical ozone profile that was only observed during summer in Boulder, Colorado, summer tends be a season where the ozone profiles become most dynamic. Though we see similar slopes to Brodin et al.'s results in colder seasons, which may validate our approach of using the two-point gradient to represent the entire ozone plume, the possibly changing ozone mechanisms at Black Hawk could still lead to bias from this approach. For example, in Brodin et al (2010)'s study, during winter the higher sites outside of the city exhibited primarily background behavior with minimal diurnal production, and this behavior changed on a multi-day scale. It is also possible the long transport distance from urban precursor sources and boundary layer isolation may sometimes result in less significant ozone increases at higher elevation, in line with our observations in summers from 2019 to 2021 (Mueller, 1994; Puxbaum et al., 1991). Therefore, because the two-point vertical gradient did not align with the observation in summer 2017, CDPHE should keep observing the

variation in this two-point gradient for a longer period or consider adding more temporary sites below the elevation of Black Hawk (2627m) to better determine the spatial and temporal behavior of ozone that Black Hawk captures.

3.3 Special event analysis–Early September 2017

Wildfire emissions are recognized to contribute both primary and secondary pollutants to the atmosphere, including carbon monoxide (CO), fine particles ($PM_{2.5}$), NO_x, volatile organic compounds, as well as ozone (Dreessen et al., 2016 and references therein). According to the investigation yielded by the Fire Influence on Regional to Global Environments and Air Quality (FIREX-AQ) study led by NOAA and NASA, ozone formation is enhanced when the presence of large amounts of VOCs are mixed into the urban plume rich with NO_x, and this effect during wildfire events is pronounced in many urban regions in Western U.S (Xu et al., 2021). The adverse health impacts of wildfire emissions also become exacerbated in the polluted urban areas (Künzli et al., 2006). A multi-day regional wildfire event in early September 2017 allowed us to examine the impact of biomass burning emissions on ozone at different elevation levels in the Denver Basin, outside of the Metropolitan Area.

According to news reports by NOAA, numerous wildfires were seen in the western United States through satellite imagery at the beginning of September, and on September 6th 65 fires were happening across the country, all of which were located in the West (Di Liberto, 2017). Local residents reported severe impacts such as reduced visibilities and falling ash. The climate conditions that aided the formation of wildfires was highlighted to be the extreme drought and hot temperatures during the summer of 2017 (Di Liberto, 2017). Wildfires in Washington, Oregon, California, Idaho, Montana, as well as western Canada were also apparent on HMS smoke product maps (Figure 16). The wildfire smoke was transported from the northwestern U.S. across much of the country, including the Colorado Front Range, and the HMS smoke product also showcases the smoke mixed down with the jet stream that was fast moving in the high atmosphere, as described in NOAA's report (Di Liberto, 2017). HYSPLIT back trajectories combined with the HMS maps to support the presence of overhead smoke in Colorado from August 27th to September 9th (Figure 16 and Figure 17). The enhanced $PM_{2.5}$

concentration of 62 μg/m^3 on September 4th measured at Chatfield Park, around 40 μg/m^3 higher than the periods before and after, confirmed the presence of smoke near the surface (Figure 18).

In the afternoons of September 4th and 6th, all sites experienced notably higher hourly ozone compared to the means of the entire study period (over mean + σ). Mines Peak spent over 10 hours each day during September 4th to 6th with hourly mixing ratios greater than 1σ above the study mean, while Jim Creek spent around 15 hours each day experiencing its mean + σ. On September 4th, Jim Creek's hourly ozone measurements exceeded 90 ppb for seven hours and, within that period, exceeded 110 ppb for four hours (Figure 20). On September 5th, all sites excluding Jim Creek and Mines Peak experienced a drop of about 20 ppb compared to the hourly measurements on the 4th, aligning with the observation earlier that suggested the similar ozone mechanisms in the lower four sites, which were separate from Jim Creek and Mines Peak. In terms of diurnal amplitudes, all sites experienced lower daily minimum ozone and thus greater amplitudes compared to that during the entire study period (around 30 ppb greater). We speculate that this might be related to the presence of smoke in this region continuously bringing in ozone precursors, adding onto the urban pollution and titrating ozone with the absence of daytime photochemistry.

MDA8 ozone during August 27th to September 9th at all sites along the vertical transect was significantly different from that during the rest of the entire study period and from that during the non-smoke days (excluding 25 smoke days). Jim Creek displayed the highest ozone mixing ratios compared to other six sites, with the average MDA8 value throughout August 27th to September 9th as 76 ppb, around 4 ppb higher than MDA8 ozone at other sites during the same period (Figure 19). The difference between Jim Creek's MDA8 during this period and during non-smoke days was also the greatest among sites, around 18 ppb, which combines to imply the greatest wildfire smoke's impact on ozone at this site. Yet Jim Creek's average MDA8 ozone during this period was not significantly different from other sites'. This suggests a regional ozone influence in the Denver Basin contributed by this prolonged presence of fire smoke.

The highest ozone measurements during this three-day period were observed under northeasterly and southeasterly winds at Centennial and Black Hawk, under easterlies at Jim Creek, and under westerlies at St. Mary (no wind data was available during this period at

Vernon). Except at St. Mary, winds coming from the east aligned with the HYSPLIT back trajectories that portray the air moving from Washington, Idaho, Montana, Wyoming, and then down to Colorado, entering the Denver Metropolitan Area from the east around September 4th (Figure 17). Windspeeds during the highest ozone period at all sites with wind data were around to below the study medians. This may suggest the stagnant airflow facilitated ozone buildup under the regional wildfire smoke. However, at Jim Creek the extremely high hourly ozone (above 100 ppb) was observed under the highest wind speed of the entire study, around 10 to 11 m/s, which can also be seen on the daytime wind rose at Jim Creek (Figure 8). The high winds from the east and the site's location on the other side of the Continental Divide, which might allow for a more direct exposure to the smoke transport from the northwest U.S., could explain why Jim Creek showed more enhanced ozone than other sites.

Thus, from this single fire event, we learned that regional wildfire smoke can enhance ozone in the Denver basin, consistent with other studies in the western U.S (Perkins, 2021). However, the varying local wind patterns may result in different levels of exposure to smoke and subsequent ozone enhancement. During this event in early September 2017, given its location in a different air shed, Jim Creek is most susceptible to the impact of wildfire smoke compared to all other sites, which may not be the case in all fire events. Trajectories with higher resolution meteorological inputs may help with determining the meteorological dynamics that led Jim Creek to experience a stronger influence of smoke, and those may also offer insights on how much the timing and the amount of wildfire emission differed among the sites (Mueller, 1994).

4. Conclusion

Results from the ozone vertical transect study in the Denver Metropolitan Area during summer 2017 demonstrate that the ozone plume likely extended up to the site Black Hawk though this site might not be the absolute height of the plume. The four lower elevation sites, NREL, Vernon, Centennial, and Black Hawk, displayed the effects of diurnal anabatic and katabatic winds coupled/ with ozone photochemical production during the day and nighttime loss. The daytime turbulent mixing within the boundary layer facilitated the transport, leading to a uniform growth in ozone mixing ratios among these lower sites in the morning. Jim Creek,

situated above these four lower sites and in a different airshed, was barely impacted by the Denver ozone plume and but showed notably higher ozone mixing ratios than the remaining sites when a major regional fire complex was present. St. Mary as another site above 3000m ASL displayed the impact of the Denver plume, but its ozone formation, accumulation, and loss may have been more driven by I-70 highway emissions. Lastly, Mines Peak, the highest and most remote site, displayed the smallest variation both diurnally and throughout the study period. Yet additional data is required to determine if it always serves as a background site in this region. As demonstrated by the varying two-point vertical gradients between NREL and Black Hawk, characterizing the Denver ozone plume is challenging with only seven sites' hourly mixing ratios in combination with wind and temperature data within a short four-month study period. Besides the multiple sources and loss processes, ozone behavior under the complex mountain-valley meteorology and terrain-induced air flow will require detailed atmospheric modeling such as GAMs and coupled chemistry-meteorology model (Jaffe and Zhang, 2017).

Given changes in global climate and the increasing frequency and severity of wildfires, long-term monitoring and analysis is necessary for implementing effective public health regulations, which can protect population in both urban and recreational areas (Barbero et al., 2015). At the same time, in addition to the dynamic natural drivers of ozone in this region, Denver as a rapidly sprawling city may have a changing landscape structure that leads to variation in urban wind ventilation and thus ozone transport mechanisms (De Wekker et al., 2018). Population growth, as another outcome of robust urban development, is also warned to be a driver for ozone pollution as emissions from motor vehicles is one of the largest local contributors to ozone (UCAR, 2017). Urban planning measures should be considered along with air quality improvement to ensure human and environmental health in the longer term.

References

Abeleira, A., Pollack, I. B., Sive, B., Zhou, Y., Fischer, E. V., & Farmer, D. K. (2017). Source characterization of volatile organic compounds in the Colorado Northern Front Range metropolitan area during spring and summer 2015. *Journal of Geophysical Research: Atmospheres*, *122*(6), 3595–3613. https://doi.org/10.1002/2016jd026227

Ambrose, J. L., Reidmiller, D. R., & Jaffe, D. A. (2011). Causes of high O3 in the lower free troposphere over the Pacific Northwest as observed at the Mt. Bachelor Observatory. *Atmospheric Environment*, *45*(30), 5302–5315. https://doi.org/10.1016/j.atmosenv.2011.06.056

Aneja, V. P., Mathur, R., Arya, S. P., Li, Y., Murray,, G. C., & Manuszak, T. L. (2000). Coupling the vertical distribution of ozone in the atmospheric boundary layer. *Environmental Science & Technology*, *34*(11), 2324–2329. https://doi.org/10.1021/es990997+

Austin, E., Zanobetti, A., Coull, B., Schwartz, J., Gold, D. R., & Koutrakis, P. (2014). Ozone trends and their relationship to characteristic weather patterns. *Journal of Exposure Science & Environmental Epidemiology*, *25*(5), 532–542. https://doi.org/10.1038/jes.2014.45

Bien, T., & Helmig, D. (2018). Changes in summertime ozone in Colorado during 2000–2015. *Elementa: Science of the Anthropocene*, *6*. https://doi.org/10.1525/elementa.300

Brodin, M., Helmig, D., & Oltmans, S. (2010). Seasonal ozone behavior along an elevation gradient in the Colorado Front Range Mountains. *Atmospheric Environment*, *44*(39), 5305–5315. https://doi.org/10.1016/j.atmosenv.2010.06.033

Brodin, M., Helmig, D., Johnson, B., & Oltmans, S. (2011). Comparison of ozone concentrations on a surface elevation gradient with balloon-borne ozonesonde measurements. *Atmospheric Environment*, *45*(31), 5431–5439. https://doi.org/10.1016/j.atmosenv.2011.07.002

Brönnimann, S., Schuepbach, E., Zanis, P., Buchmann, B., & Wanner, H. (2000). A climatology of regional background ozone at different elevations in Switzerland (1992–1998). *Atmospheric Environment*, *34*(29-30), 5191–5198. https://doi.org/10.1016/s1352-2310(00)00193-x

Bytnerowicz, A., Godzik, B., Frączek, W., Grodzińska, K., Krywult, M., Badea, O., Barančok, P., Blum, O., Černy, M., Godzik, S., Mankovska, B., Manning, W., Moravčik, P., Musselman, R., Oszlanyi, J., Postelnicu, D., Szdźuj, J., Varšavova, M., & Zota, M. (2002). Distribution of ozone and other air pollutants in forests of the Carpathian Mountains in Central Europe. *Environmental Pollution*, *116*(1), 3–25. https://doi.org/10.1016/s0269-7491(01)00187-7

Camalier, L., Cox, W., & Dolwick, P. (2007). The effects of meteorology on ozone in urban areas and their use in assessing ozone trends. *Atmospheric Environment*, *41*(33), 7127–7137. https://doi.org/10.1016/j.atmosenv.2007.04.061

Caputi, D. J., Faloona, I., Trousdell, J., Smoot, J., Falk, N., & Conley, S. (2019). Residual layer ozone, mixing, and the nocturnal jet in California's San Joaquin Valley. *Atmospheric Chemistry and Physics*, *19*(7), 4721–4740. https://doi.org/10.5194/acp-19-4721-2019

Chevalier, A., Gheusi, F., Delmas, R., Ordóñez, C., Sarrat, C., Zbinden, R., Thouret, V., Athier, G., & Cousin, J.-M. (2007). Influence of altitude on ozone levels and variability in the lower troposphere: A ground-based study for Western Europe over the period 2001–2004. *Atmospheric Chemistry and Physics*, *7*(16), 4311–4326. https://doi.org/10.5194/acp-7-4311-2007

Chevalier, A., Gheusi, F., Delmas, R., Ordóñez, C., Sarrat, C., Zbinden, R., Thouret, V., Athier, G., & Cousin, J.-M. (2007). Influence of altitude on ozone levels and variability in the lower troposphere: A ground-based study for Western Europe over the period 2001–2004. *Atmospheric Chemistry and Physics*, *7*(16), 4311–4326. https://doi.org/10.5194/acp-7-4311-2007

Conley, S. A., Faloona, I. C., Lenschow, D. H., Campos, T., Heizer, C., Weinheimer, A., Cantrell, C. A., Mauldin, R. L., Hornbrook, R. S., Pollack, I., & Bandy, A. (2011). A complete dynamical ozone budget measured in the tropical marine boundary layer during Pase. *Journal of Atmospheric Chemistry*, *68*(1), 55–70. https://doi.org/10.1007/s10874-011-9195-0

Cooper, O. R., Langford, A. O., Parrish, D. D., & Fahey, D. W. (2015). Challenges of a lowered U.S. Ozone Standard. *Science*, *348*(6239), 1096–1097. https://doi.org/10.1126/science.aaa5748

Cooper, O. R., Oltmans, S. J., Johnson, B. J., Brioude, J., Angevine, W., Trainer, M., Parrish, D. D., Ryerson, T. R., Pollack, I., Cullis, P. D., Ives, M. A., Tarasick, D. W., Al-Saadi, J., & Stajner, I. (2011). Measurement of western U.S. baseline ozone from the surface to the tropopause and assessment of downwind impact regions. *Journal of Geophysical Research: Atmospheres*, *116*(D21). https://doi.org/10.1029/2011jd016095

Cooper, O. R., Parrish, D. D., Ziemke, J., Balashov, N. V., Cupeiro, M., Galbally, I. E., Gilge, S., Horowitz, L., Jensen, N. R., Lamarque, J.-F., Naik, V., Oltmans, S. J., Schwab, J., Shindell, D. T., Thompson, A. M., Thouret, V., Wang, Y., & Zbinden, R. M. (2014). Global distribution and trends of tropospheric ozone: An observation-based review. *Elementa: Science of the Anthropocene*, *2*. https://doi.org/10.12952/journal.elementa.000029

Cooper, S. M., & Peterson, D. L. (2000). Spatial distribution of tropospheric ozone in Western Washington, USA. *Environmental Pollution*, *107*(3), 339–347. https://doi.org/10.1016/s0269-7491(99)00172-4

Crawford, J. H., Davis, D. D., Chen, G., Buhr, M., Oltmans, S., Weller, R., Mauldin, L., Eisele, F., Shetter, R., Lefer, B., Arimoto, R., & Hogan, A. (2001). Evidence for photochemical production of ozone at the South Pole Surface. *Geophysical Research Letters*, *28*(19), 3641–3644. https://doi.org/10.1029/2001gl013055

Crooks, J. L., Licker, R., Hollis, A. L., & Ekwurzel, B. (2021). The ozone climate penalty, Naaqs attainment, and health equity along the Colorado Front Range. *Journal of Exposure Science & Environmental Epidemiology*. https://doi.org/10.1038/s41370-021-00375-9

De Wekker, S., Kossmann, M., Knievel, J., Giovannini, L., Gutmann, E., & Zardi, D. (2018). Meteorological applications benefiting from an improved understanding of atmospheric exchange processes over mountains. *Atmosphere*, *9*(10), 371. https://doi.org/10.3390/atmos9100371

Demographics. Demographics | Metro Denver. (n.d.). Retrieved March 12, 2022, from https://www.metrodenver.org/regional-data/demographics

Dreessen, J., Sullivan, J., & Delgado, R. (2016). Observations and impacts of transported Canadian wildfire smoke on ozone and aerosol air quality in the Maryland region on June 9–12, 2015. *Journal of the Air & Waste Management Association*, *66*(9), 842–862. https://doi.org/10.1080/10962247.2016.1161674

Di Liberto, T. (2017, September 7). *Massive fires burning across the West in September 2017*. Massive fires burning across the West in September 2017 | NOAA Climate.gov. Retrieved March 30, 2022, from https://www.climate.gov/news-features/event-tracker/massive-fires-burning-across-west-september-2017

Evans, J. M., & Helmig, D. (2016). Investigation of the influence of transport from oil and natural gas regions on elevated ozone levels in the Northern Colorado Front Range. *Journal of the Air & Waste Management Association*, *67*(2), 196–211. https://doi.org/10.1080/10962247.2016.1226989

Felzer, B. S., Cronin, T., Reilly, J. M., Melillo, J. M., & Wang, X. (2007). Impacts of ozone on trees and crops. *Comptes Rendus Geoscience*, *339*(11-12), 784–798. https://doi.org/10.1016/j.crte.2007.08.008

Fine, R., Miller, M. B., Burley, J., Jaffe, D. A., Pierce, R. B., Lin, M., & Gustin, M. S. (2015). Variability and sources of surface ozone at rural sites in Nevada, USA: Results from two years of the Nevada Rural Ozone Initiative. *Science of The Total Environment*, *530-531*, 471–482. https://doi.org/10.1016/j.scitotenv.2014.12.027

Flocke, F., Pfister, G., Crawford, J. H., Pickering, K. E., Pierce, G., Bon, D., & Reddy, P. (2020). Air Quality in the Northern Colorado Front Range Metro Area: The Front Range Air Pollution and photochemistry éxperiment (FRAPPÉ). *Journal of Geophysical Research: Atmospheres*, *125*(2). https://doi.org/10.1029/2019jd031197

Flynn, M. T., Mattson, E. J., Jaffe, D. A., & Gratz, L. E. (2021). Spatial patterns in summertime surface ozone in the Southern Front Range of the U.S. rocky mountains. *Elementa: Science of the Anthropocene*, *9*(1). https://doi.org/10.1525/elementa.2020.00104

Gong, X., Kaulfus, A., Nair, U., & Jaffe, D. A. (2017). Quantifying O3 impacts in urban areas due to wildfires using a generalized additive model. *Environmental Science & Technology*, *51*(22), 13216–13223. https://doi.org/10.1021/acs.est.7b03130

Helmig, D., Johnson, B., Oltmans, S., Neff, W., Eisele, F., & Davis, D. (2008). Elevated ozone in the boundary layer at South Pole. *Atmospheric Environment*, *42*(12), 2788–2803. https://doi.org/10.1016/j.atmosenv.2006.12.032

Hu, J., Li, Y., Zhao, T., Liu, J., Hu, X.-M., Liu, D., Jiang, Y., Xu, J., & Chang, L. (2018). An important mechanism of regional O3 transport for summer smog over the Yangtze River Delta in eastern China. *Atmospheric Chemistry and Physics*, *18*(22), 16239–16251. https://doi.org/10.5194/acp-18-16239-2018

Jaffe, D. (2010). Relationship between surface and free tropospheric ozone in the western U.S. *Environmental Science & Technology*, *45*(2), 432–438. https://doi.org/10.1021/es1028102

Jaffe, D. A., & Zhang, L. (2017). Meteorological anomalies lead to elevated O 3 in the western U.S. in June 2015. *Geophysical Research Letters*, *44*(4), 1990–1997. https://doi.org/10.1002/2016gl072010

Jaffe, D. A., Cooper, O. R., Fiore, A. M., Henderson, B. H., Tonnesen, G. S., Russell, A. G., Henze, D. K., Langford, A. O., Lin, M., & Moore, T. (2018). Scientific assessment of background ozone over the U.S.: Implications for air quality management. *Elementa: Science of the Anthropocene*, *6*. https://doi.org/10.1525/elementa.309

Kaser, L., Patton, E. G., Pfister, G. G., Weinheimer, A. J., Montzka, D. D., Flocke, F., Thompson, A. M., Stauffer, R. M., & Halliday, H. S. (2017). The effect of entrainment through atmospheric boundary layer growth on observed and modeled surface ozone in the Colorado Front Range. *Journal of Geophysical Research: Atmospheres*, *122*(11), 6075–6093. https://doi.org/10.1002/2016jd026245

Künzli, N., Avol, E., Wu, J., Gauderman, W. J., Rappaport, E., Millstein, J., Bennion, J., McConnell, R., Gilliland, F. D., Berhane, K., Lurmann, F., Winer, A., & Peters, J. M. (2006). Health effects of the 2003 Southern California wildfires on children. *American Journal of Respiratory and Critical Care Medicine*, *174*(11), 1221–1228. https://doi.org/10.1164/rccm.200604-519oc

Langford, A. O., Alvarez, R. J., Brioude, J., Fine, R., Gustin, M. S., Lin, M. Y., Marchbanks, R. D., Pierce, R. B., Sandberg, S. P., Senff, C. J., Weickmann, A. M., & Williams, E. J. (2017). Entrainment of stratospheric air and Asian pollution by the convective boundary layer in the southwestern U.S. *Journal of Geophysical Research: Atmospheres*, *122*(2), 1312–1337. https://doi.org/10.1002/2016jd025987

Lehning, M., Richner, H., Kok, G. L., & Neininger, B. (1998). Vertical Exchange and regional budgets of air pollutants over densely populated areas. *Atmospheric Environment*, *32*(8), 1353–1363. https://doi.org/10.1016/s1352-2310(97)00249-5

Xu, L., Crounse, J. D., Vasquez, K. T., Allen, H., Wennberg, P. O., Bourgeois, I., Brown, S. S., Campuzano-Jost, P., Coggon, M. M., Crawford, J. H., DiGangi, J. P., Diskin, G. S., Fried, A., Gargulinski, E. M., Gilman, J. B., Gkatzelis, G. I., Guo, H., Hair, J. W., Hall, S. R., Halliday, H. A., Hanisco, T. F., Hannun, R. A., Holmes, C. D., Huey, L. G., Jimenez, J. L. (2021). Ozone Chemistry in western U.S. wildfire plumes. Science advances. Science Advances, 50(7). https://doi.org/10.1126/sciadv.abl3648

Mattson, E., & Stauffer, P. (n.d.). Ozone Special Study in Grand Junction, Colorado, Summer 2016. Colorado Air Pollution Control Division.

McClure, C. D., & Jaffe, D. A. (2018). Investigation of high ozone events due to wildfire smoke in an urban area. *Atmospheric Environment*, *194*, 146–157. https://doi.org/10.1016/j.atmosenv.2018.09.021

McDonald-Buller, E. C., Allen, D. T., Brown, N., Jacob, D. J., Jaffe, D., Kolb, C. E., Lefohn, A. S., Oltmans, S., Parrish, D. D., Yarwood, G., & Zhang, L. (2011). Establishing policy relevant background (PRB) ozone concentrations in the United States. *Environmental Science & Technology*, *45*(22), 9484–9497. https://doi.org/10.1021/es2022818

Monks, P. S., Salisbury, G., Holland, G., Penkett, S. A., & Ayers, G. P. (2000). A seasonal comparison of ozone photochemistry in the remote marine boundary layer. *Atmospheric Environment*, *34*(16), 2547–2561. https://doi.org/10.1016/s1352-2310(99)00504-x

Mueller, S. F. (1994). Characterization of ambient ozone levels in the Great Smoky Mountains National Park. *Journal of Applied Meteorology*, *33*(4), 465–472. https://doi.org/10.1175/1520-0450(1994)033<0465:coaoli>2.0.co;2

Musselman, R., Lefohn, A., Massman, W., & Heath, R. (2006). A critical review and analysis of the use of exposure- and flux-based ozone indices for predicting vegetation effects. *Atmospheric Environment*, *40*(10), 1869–1888. https://doi.org/10.1016/j.atmosenv.2005.10.064

NOAA Air Resources Laboratory. (2022, January 4). The HYSPLIT model. Retrieved March 30, 2022, from https://www.ready.noaa.gov/HYSPLIT.php.

Oldham, J. (2020, February 11). *Instead of releasing this greenhouse gas, beer brewers are selling it to pot growers*. The Washington Post. Retrieved April 20, 2022, from https://www.washingtonpost.com/climate-solutions/instead-of-releasing-this-greenhouse-gas-beer-brewers-are-selling-it-to-pot-growers/2020/02/11/cf1410ae-49c3-11ea-b4d9-29cc419287eb_story.html

Oltmans, S. J., Cheadle, L. C., Johnson, B. J., Schnell, R. C., Helmig, D., Thompson, A. M., Cullis, P., Hall, E., Jordan, A., Sterling, C., McClure-Begley, A., Sullivan, J. T., McGee, T. J., & Wolfe, D. (2019). Boundary layer ozone in the Northern Colorado Front Range in July–August 2014 during Frappe and discover-aq from vertical profile measurements. *Elementa: Science of the Anthropocene*, *7*. https://doi.org/10.1525/elementa.345

Perkins, R. (2021, December 8). *Scientists show how wildfire smoke increases ozone pollution*. California Institute of Technology. Retrieved April 20, 2022, from https://www.caltech.edu/about/news/scientists-show-how-wildfire-smoke-increases-ozone-pollution#:~:text=%22%20Wildfires%20increase%20regional%20ozone%20across,few%20years%2C%22%20says%20Xu.

Pfister, G. G., Reddy, P. J., Barth, M. C., Flocke, F. F., Fried, A., Herndon, S. C., Sive, B. C., Sullivan, J. T., Thompson, A. M., Yacovitch, T. I., Weinheimer, A. J., & Wisthaler, A. (2017). Using observations and source-specific model tracers to characterize pollutant transport during FRAPPÉ and discover-aq. *Journal of Geophysical Research: Atmospheres*, *122*(19). https://doi.org/10.1002/2017jd027257

Pfister, G., Wang, C. T., Barth, M., Flocke, F., Vizuete, W., & Walters, S. (2019). Chemical characteristics and ozone production in the Northern Colorado Front Range. *Journal of Geophysical Research: Atmospheres*, *124*(23), 13397–13419. https://doi.org/10.1029/2019jd030544

Puxbaum, H., Gabler, K., Smidt, S., & Glattes, F. (1991). A one-year record of ozone profiles in an Alpine Valley (Zillertal/Tyrol, Austria, 600–2000 m a.s.l.). *Atmospheric Environment. Part A. General Topics*, *25*(9), 1759–1765. https://doi.org/10.1016/0960-1686(91)90260-e

Ribas, A., & Penuelas, J. (2006). Surface ozone mixing ratio increase with altitude in a transect in the Catalan Pyrenees. *Atmospheric Environment*, *40*(38), 7308–7315. https://doi.org/10.1016/j.atmosenv.2006.06.039

Ribas, À., & Peñuelas, J. (2004). Temporal patterns of surface ozone levels in different habitats of the north western Mediterranean Basin. *Atmospheric Environment*, *38*(7), 985–992. https://doi.org/10.1016/j.atmosenv.2003.10.045

Schnell, R. C., Oltmans, S. J., Neely, R. R., Endres, M. S., Molenar, J. V., & White, A. B. (2009). Rapid photochemical production of ozone at high concentrations in a rural site during winter. *Nature Geoscience*, *2*(2), 120–122. https://doi.org/10.1038/ngeo415

Simon, H., Reff, A., Wells, B., Xing, J., & Frank, N. (2014). Ozone trends across the United States over a period of decreasing NOx and VOC emissions. *Environmental Science & Technology*, *49*(1), 186–195. https://doi.org/10.1021/es504514z

Steiner, A. L., Davis, A. J., Sillman, S., Owen, R. C., Michalak, A. M., & Fiore, A. M. (2010). Observed suppression of ozone formation at extremely high temperatures due to chemical and biophysical feedbacks. *Proceedings of the National Academy of Sciences*, *107*(46), 19685–19690. https://doi.org/10.1073/pnas.1008336107

State of Colorado. (n.d.). *Greening the Cannabis Industry*. Colorado Department of Public Health & Environment. Retrieved April 20, 2022, from https://cdphe.colorado.gov/greening-the-cannabis-industry

Strode, S. A., Rodriguez, J. M., Logan, J. A., Cooper, O. R., Witte, J. C., Lamsal, L. N., Damon, M., Van Aartsen, B., Steenrod, S. D., & Strahan, S. E. (2015). Trends and variability in surface ozone over the United States. *Journal of Geophysical Research: Atmospheres*, *120*(17), 9020–9042. https://doi.org/10.1002/2014jd022784

Stull, R. B. (2009). *An introduction to boundary layer meteorology*. Springer.

Thompson, T. M. (2019, January 31). *Background ozone: Challenges in science and policy*. Congressional Research Service. Retrieved March 8, 2022, from https://crsreports.congress.gov/product/pdf/R/R45482

Toth, J. J., & Johnson, R. H. (1985). Summer surface flow characteristics over Northeast Colorado. *Monthly Weather Review*, *113*(9), 1458–1469. https://doi.org/10.1175/1520-0493(1985)113<1458:ssfcon>2.0.co;2

Trousdell, J. F., Conley, S. A., Post, A., & Faloona, I. C. (2016). Observing entrainment mixing, photochemical ozone production, and regional methane emissions by aircraft using a simple mixed-layer framework. *Atmospheric Chemistry and Physics*, *16*(24), 15433–15450. https://doi.org/10.5194/acp-16-15433-2016

UCAR. (2017, October 30). *Scientists pinpoint sources of Front Range Ozone*. NCAR & UCAR News. Retrieved April 18, 2022, from https://news.ucar.edu/129774/scientists-pinpoint-sources-front-range-ozone

US EPA.

a. (n.d.). Ground-level Ozone Basics. Retrieved March 9, 2022, from https://www.epa.gov/ground-level-ozone-pollution/ground-level-ozone-basics#formation
b. (n.d.). 2008 Ozone National Ambient Air Quality Standards (NAAQS) Nonattainment Actions. Retrieved April 17, 2022, from https://www.epa.gov/ground-level-ozone-pollution/2008-ozone-national-ambient-air-quality-standards-naaqs-nonattainment
c. (2021, January). 2017 National Emissions Inventory (NEI) Data. Retrieved March 30, 2022, from https://www.epa.gov/air-emissions-inventories/2017-national-emissions-inventory-nei-data.
d. (2021, November 24). Pre-Generated Data Files - Particulates. Retrieved March 30, 2022, from https://aqs.epa.gov/aqsweb/airdata/download_files.html#Daily.

Wang, S., Ackermann, R., & Stutz, J. (2006). Vertical profiles of O3 and NOx chemistry in the polluted nocturnal boundary layer in Phoenix, AZ: I. Field observations by long-path DOAS. *Atmospheric Chemistry and Physics*, *6*(9), 2671–2693. https://doi.org/10.5194/acp-6-2671-2006

Wesely, M., & Hicks, B. B. (2000). A review of the current status of knowledge on dry deposition. *Atmospheric Environment*, *34*(12-14), 2261–2282. https://doi.org/10.1016/s1352-2310(99)00467-7

Figures and Tables

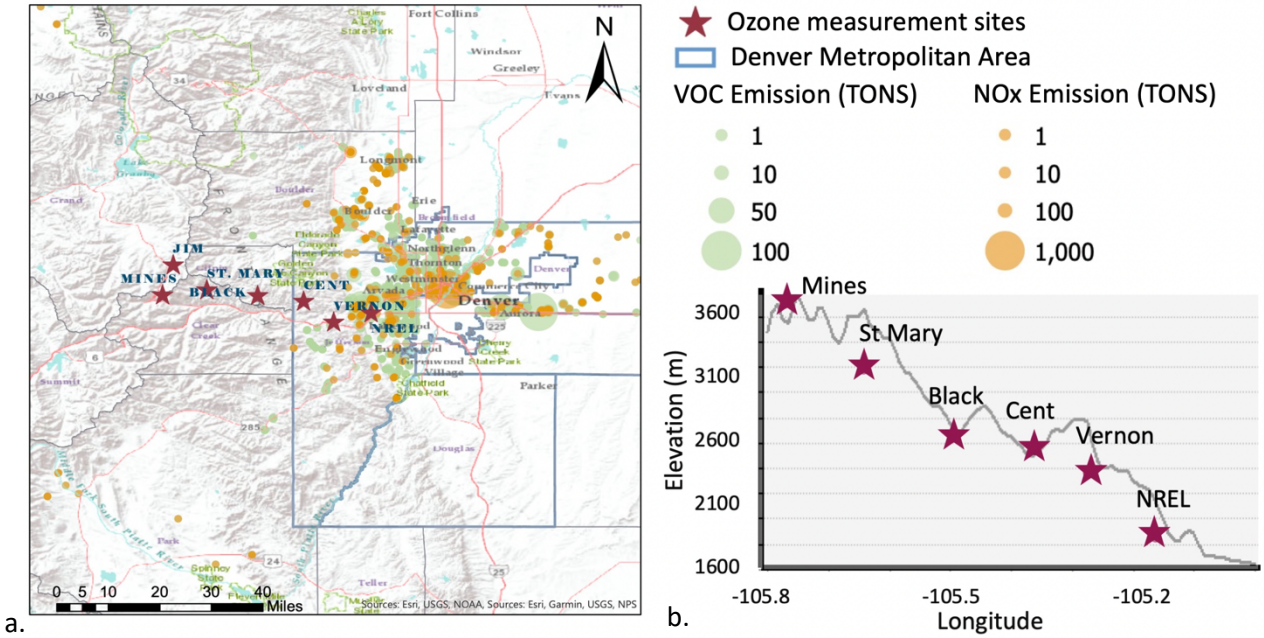

Figure 1 a) Map of study area that shows stationary ozone precursor emission sources, and the study measurement sites that included three long-term permanent sites NREL, Black Hawk (Black), and Mines, and four temporary sites, Vernon, Centennial (Cent), St. Mary, and Jim Creek (Jim). b) Graphical representation of the elevation transect excluding Jim Creek because of its location in a different air shed.

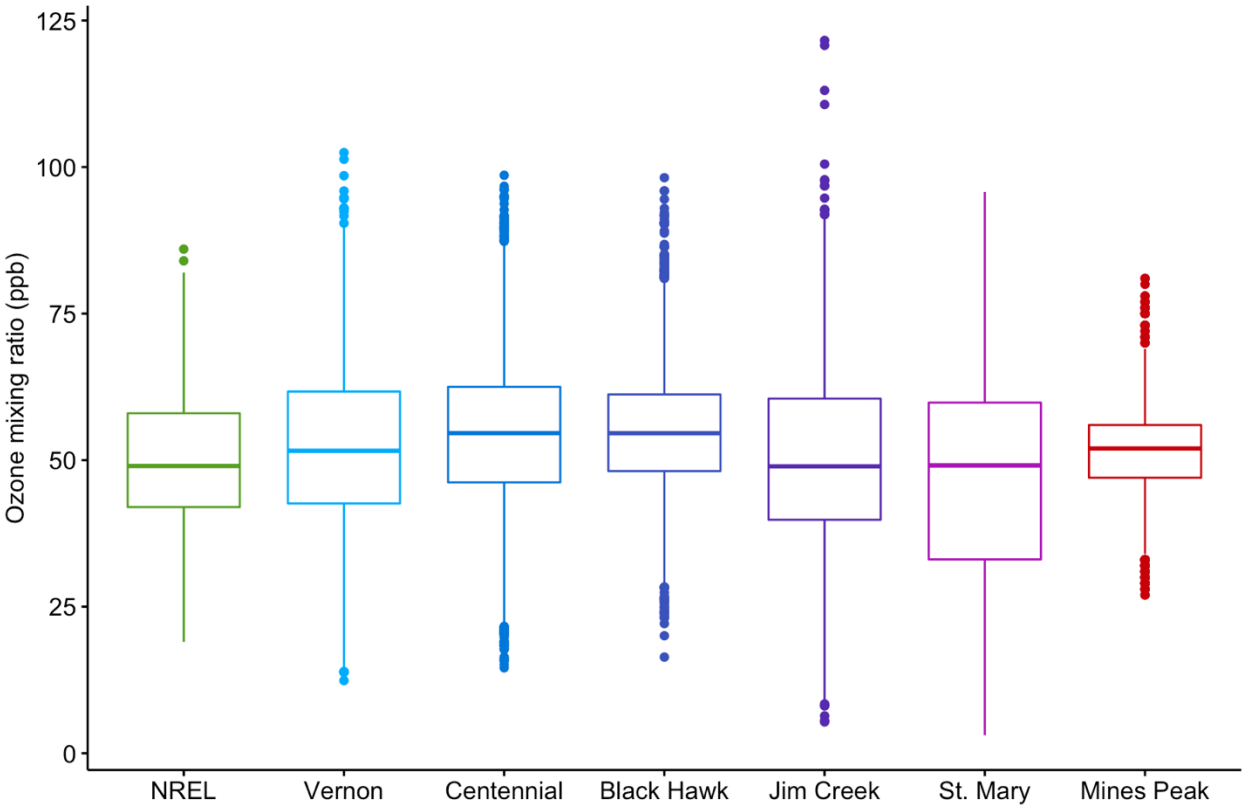

Figure 2. Boxplot distribution of all sites' hourly ozone measurements throughout the June-September 2017 study period. The boxes represent median, 25th and 75th percentile. The colors correspond to the order of elevation along the transect. The upper and lower whiskers represent the maximum and minimum values of the hourly measurement, or the upper and lower quartile plus and minus 1.5 * Interquartile Range.

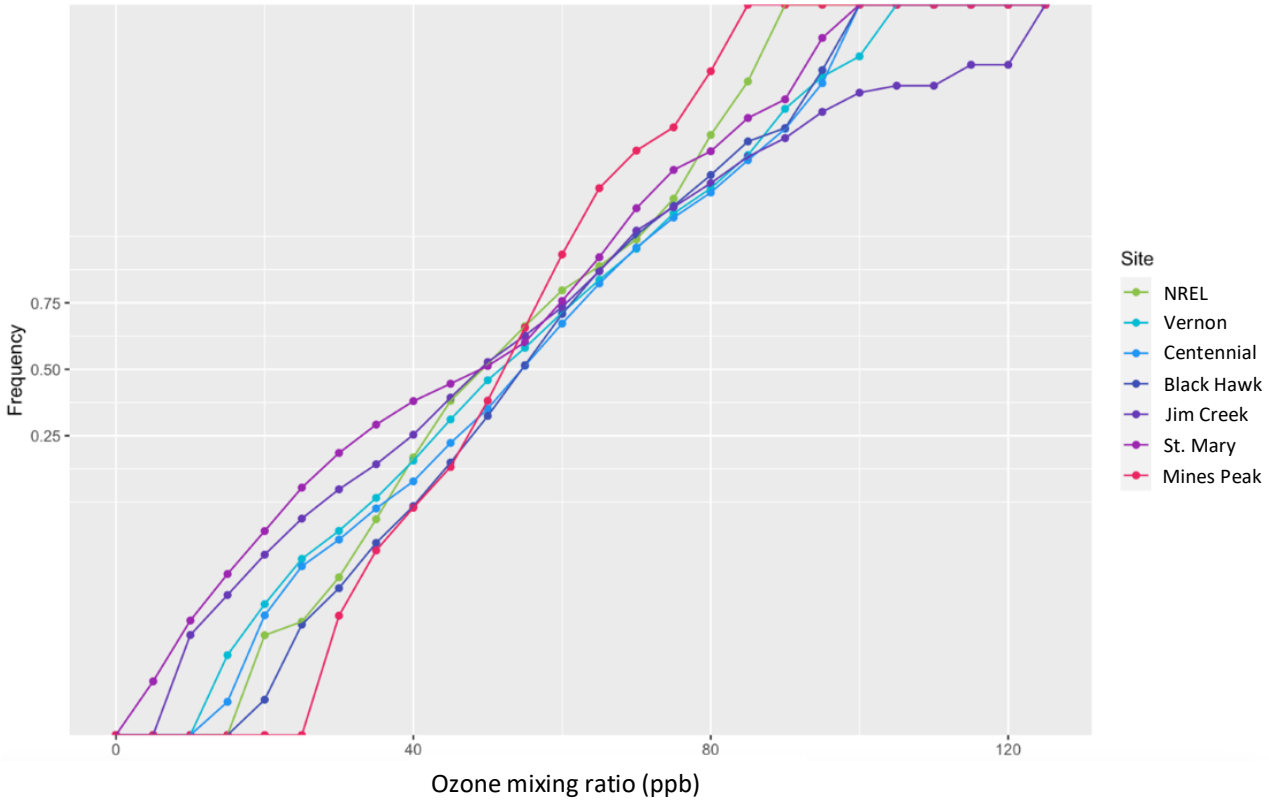

Figure 3. Cumulative frequency plot of all sites' hourly ozone measurements throughout the entire study period. The vertical scale is logarithmic, and the upper and lower tick marks are each close to 1.0 and 0.

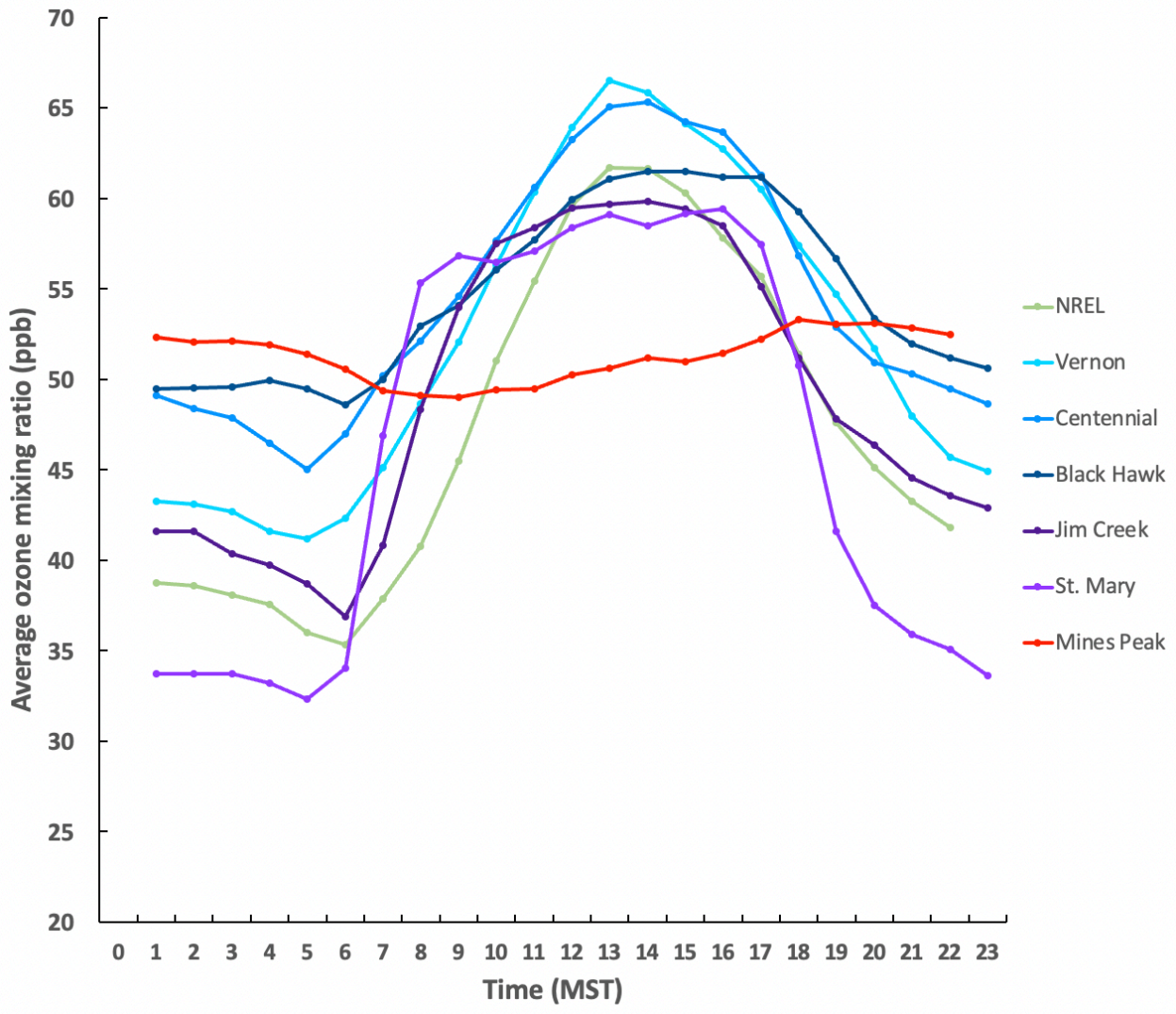

Figure 4. Average hourly ozone mixing ratios throughout the entire study periods at all seven sites.

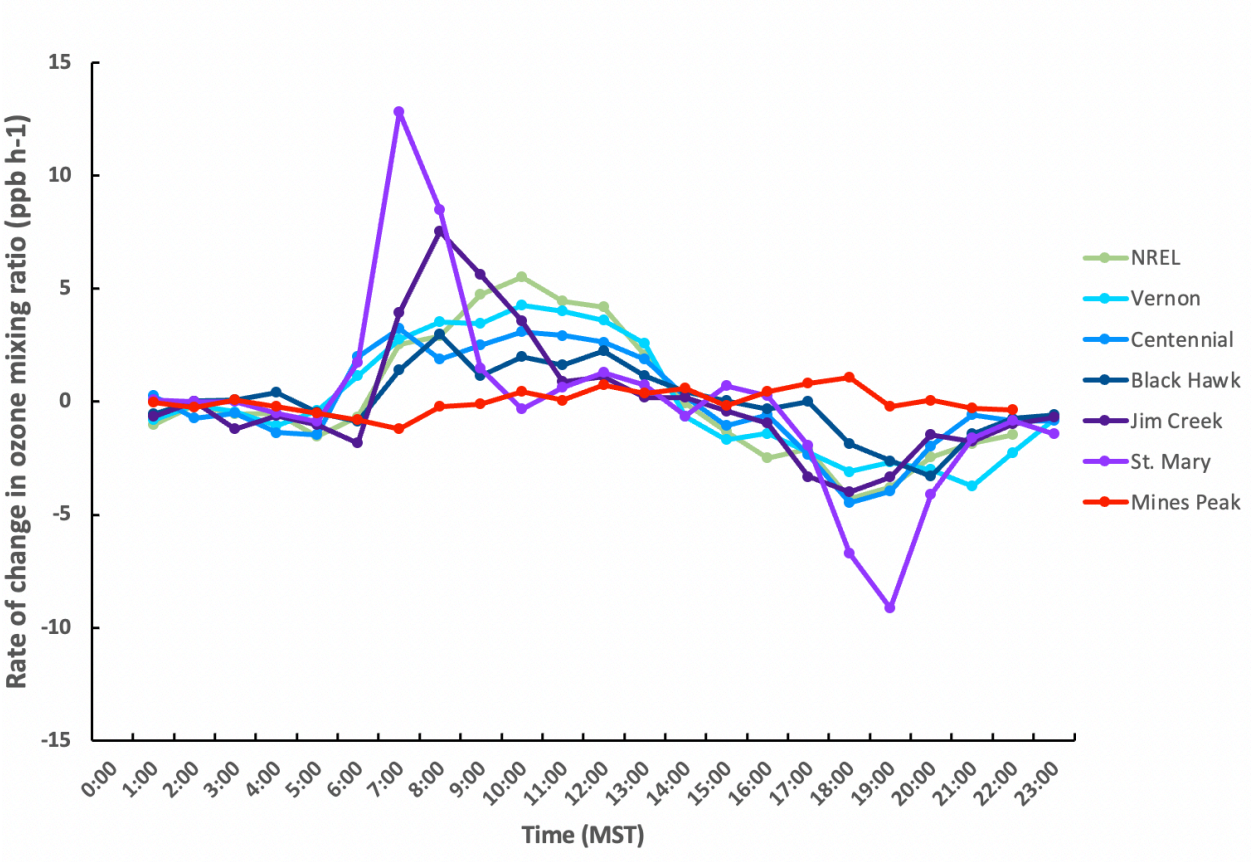

Figure 5. Average rate of change of hourly ozone mixing ratios throughout the entire study periods at all sites.

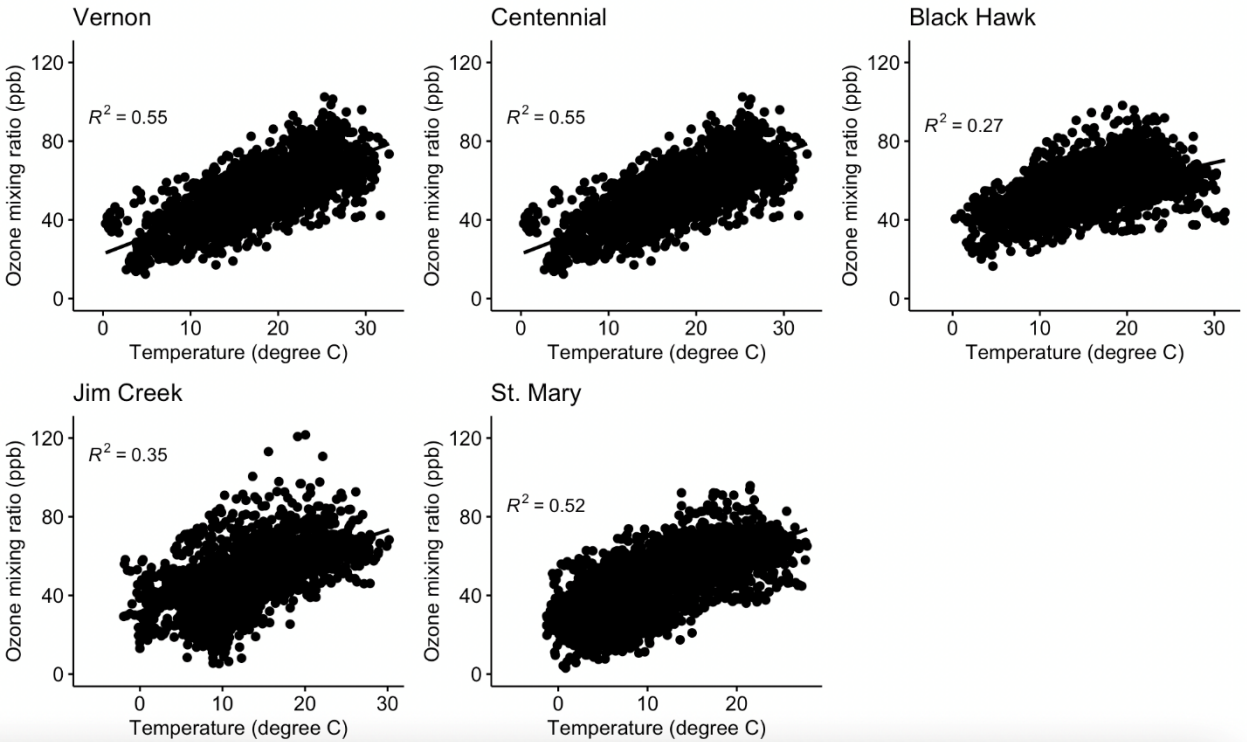

Figure 6. Pearson correlations between ozone mixing ratio and temperature at Vernon, Centennial, Black Hawk, Jim Creek, and St. Mary ($p << 0.0001$).

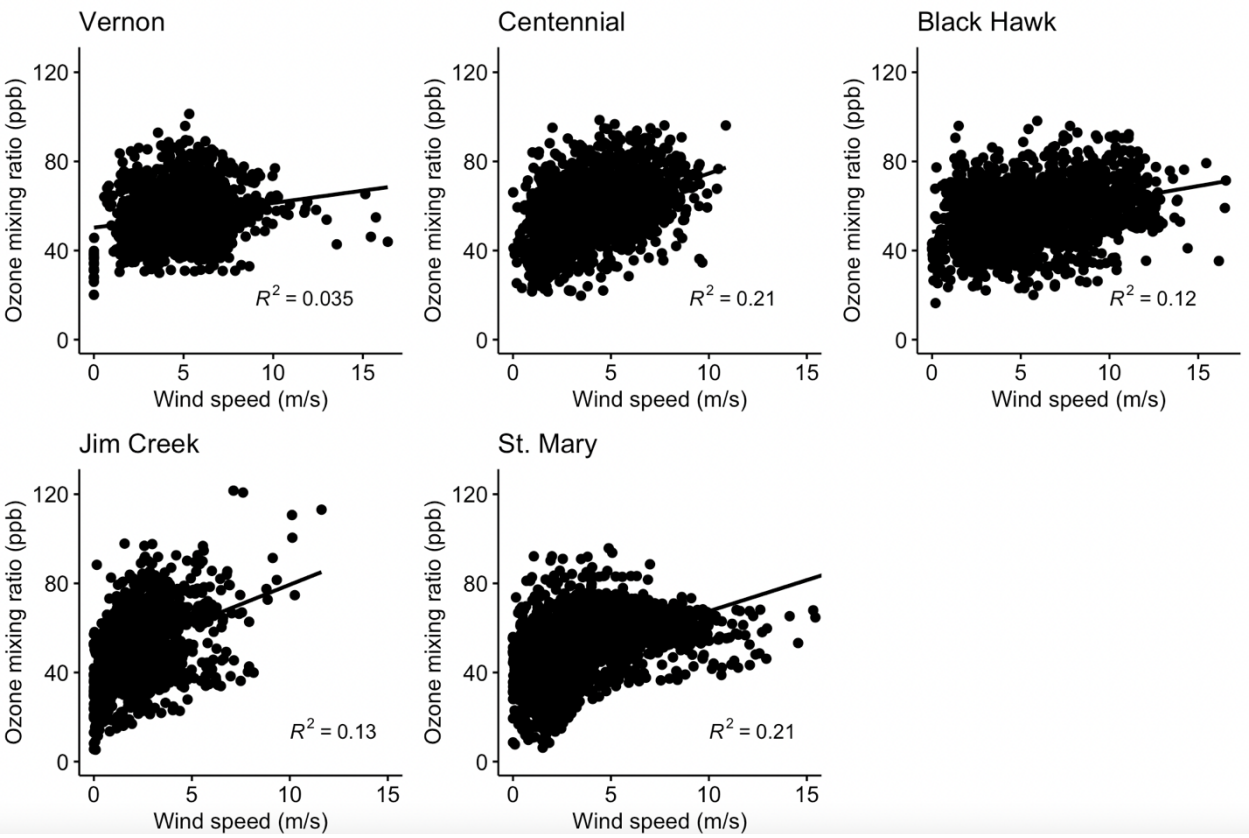

Figure 7. Pearson correlations between ozone mixing ratio and wind speed at Vernon, Centennial, Black Hawk, Jim Creek, and St. Mary ($p<<0.0001$).

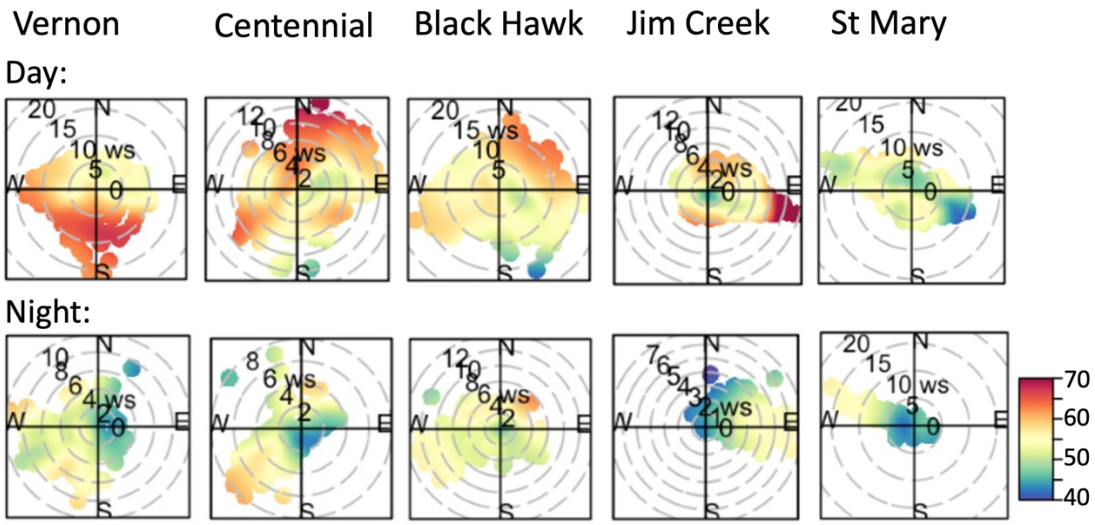

Figure 8. Diurnal wind roses at Vernon, Centennial, Black Hawk, Jim Creek, and St Mary. The scale bar represents the hourly ozone mixing ratios in ppb. Note that the scales for wind speed are not consistent between figures.

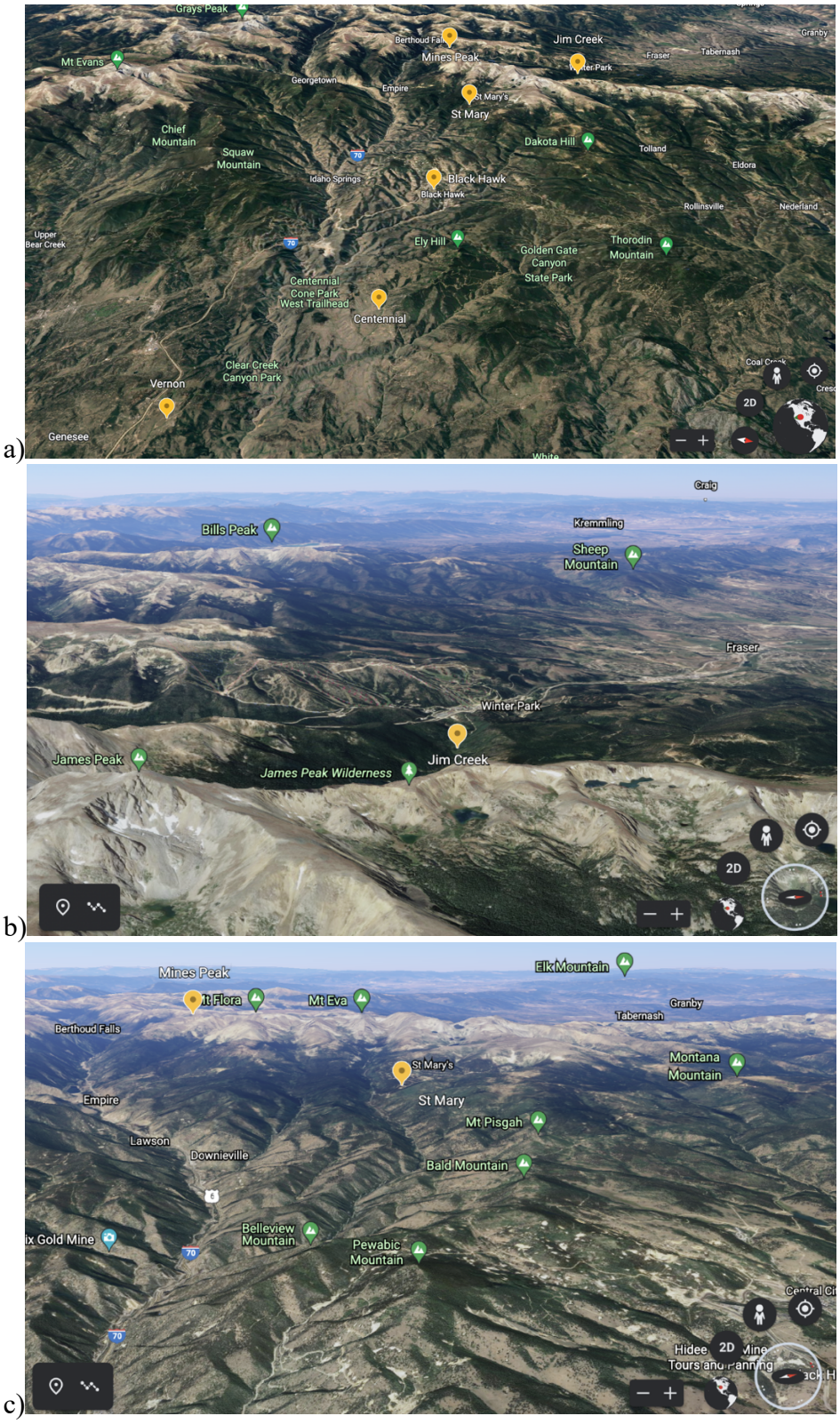

Figure 9. Local topography with the viewing angle from the east a) along the transect starting from Vernon to Mines Peak, b) near Jim Creek, and c) near St. Mary.

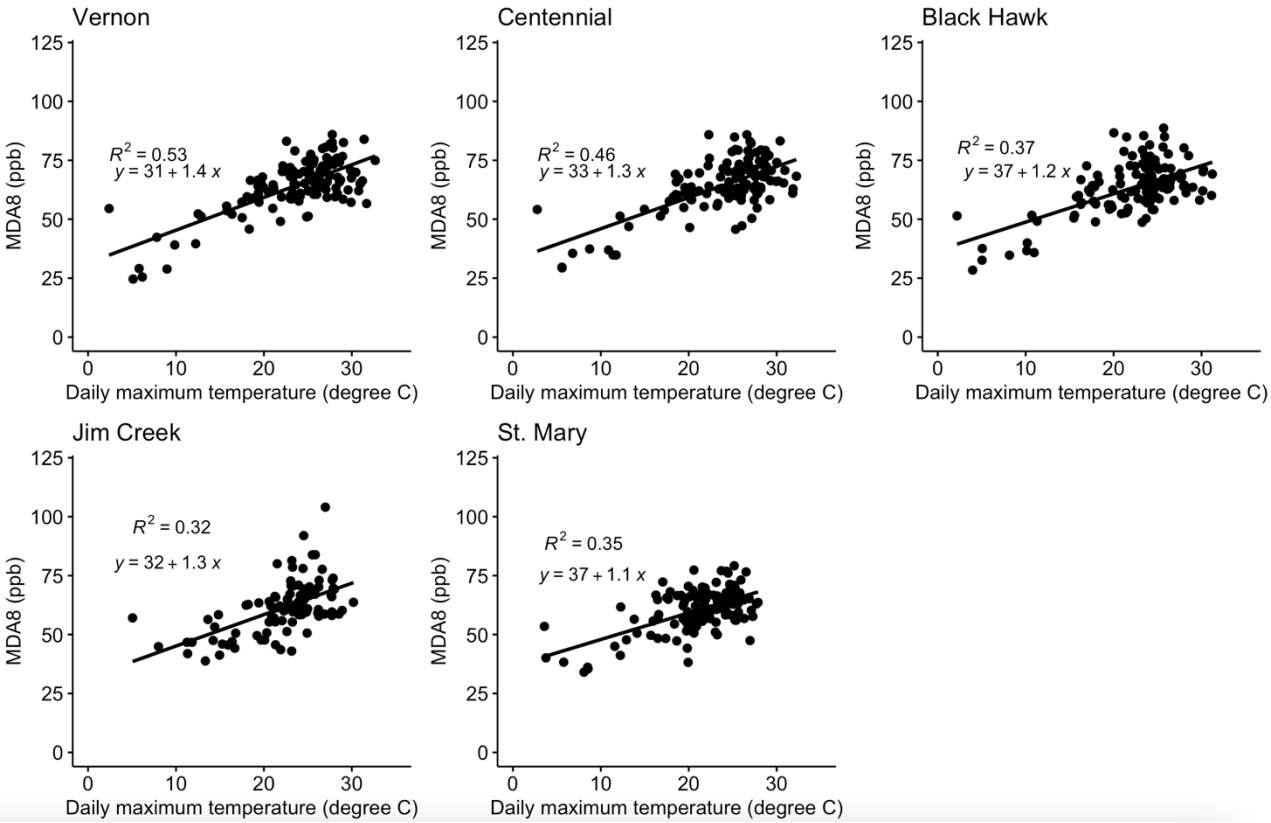

Figure 10. Pearson correlations between MDA8 ozone mixing ratio and daily maximum temperature at Vernon, Centennial, Black Hawk, Jim Creek, and St. Mary ($p<<0.0001$).

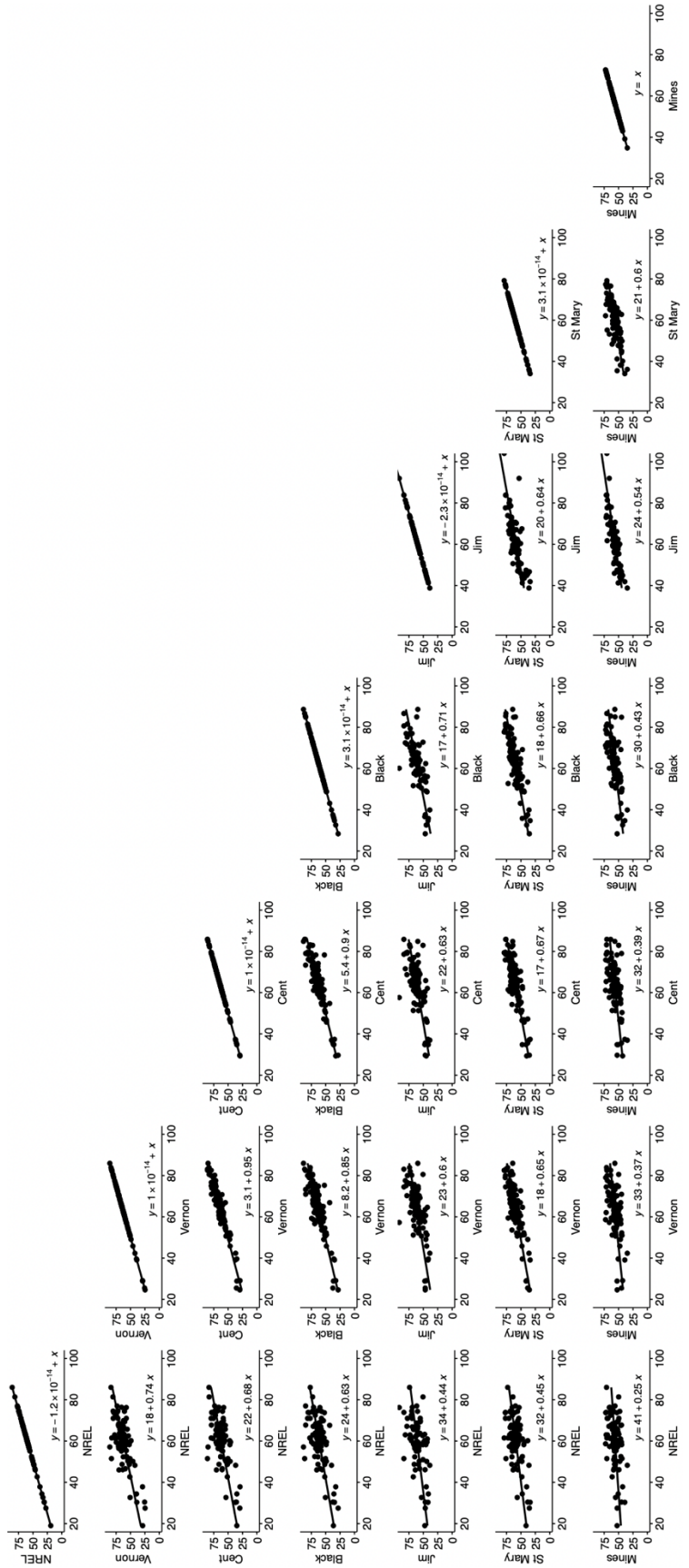

Figure 11. Pearson pair-wise correlations among all sites' MDA8 values with regression slopes.

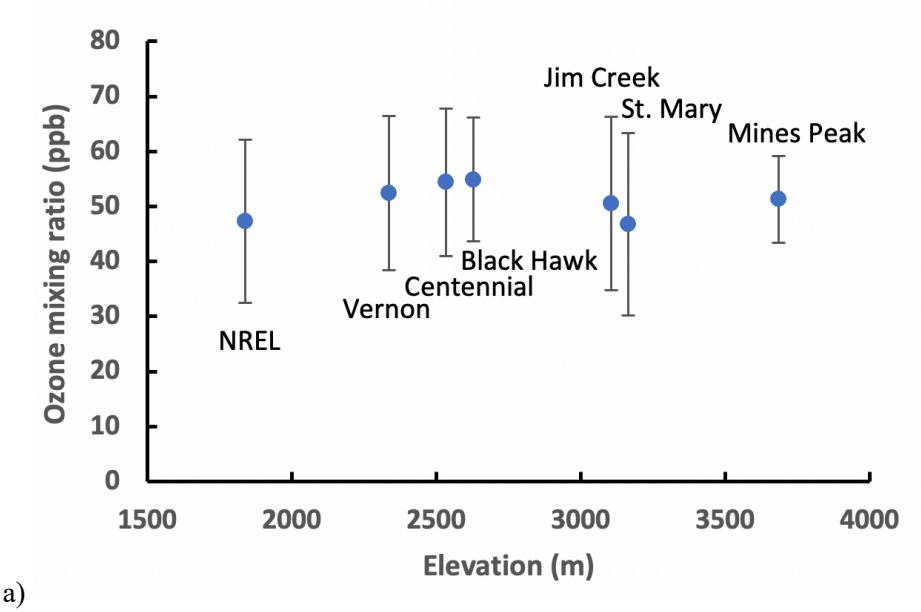

a)

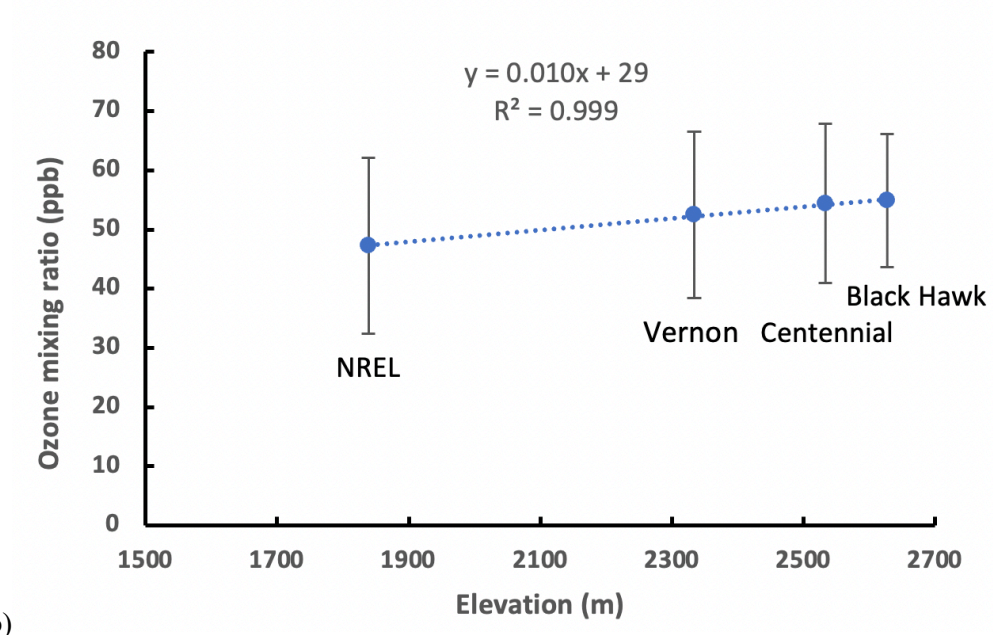

b)

Figure 12. a) Average ozone mixing ratios against elevation at all sites with error bars representing standard deviations. b) Regression between average ozone mixing ratios and elevation among the lower four sites, from NREL to Black Hawk.

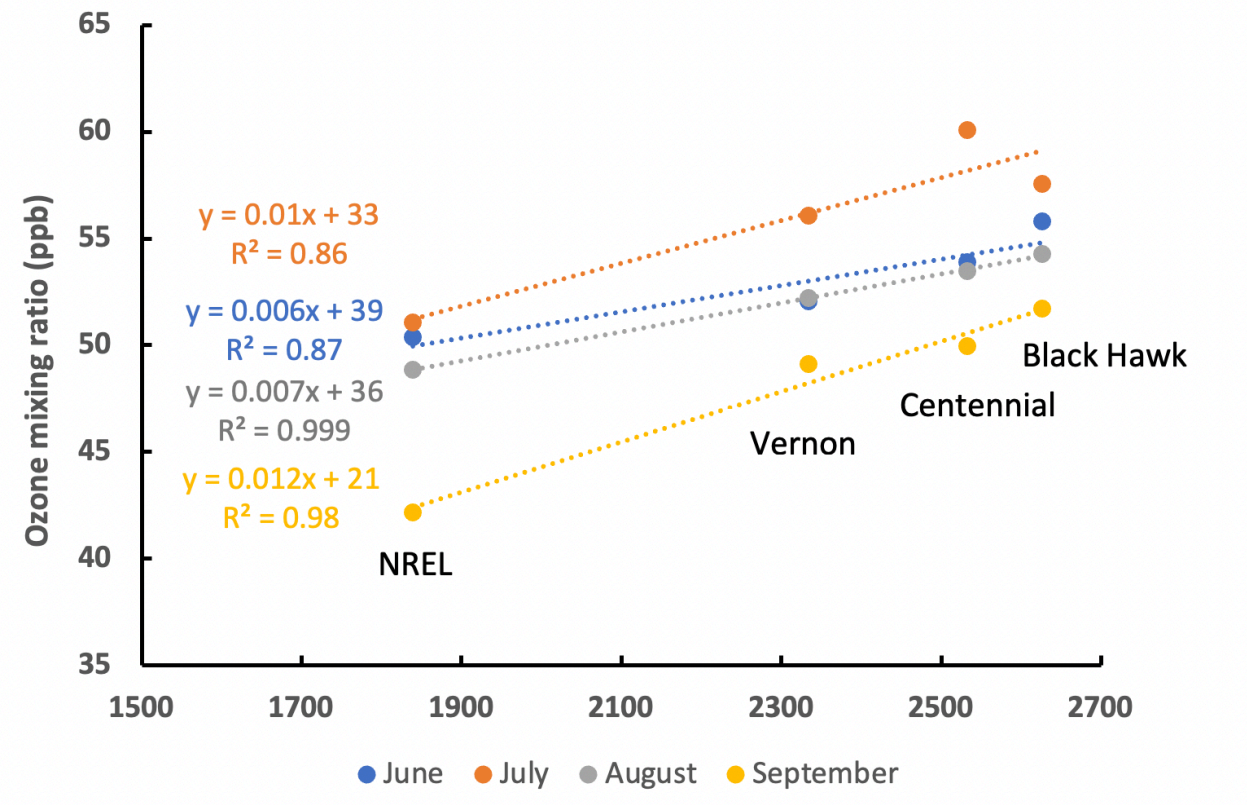

Figure 13. Monthly average ozone gradient with elevation among four lower sites, NREL, Vernon, Centennial, and Black Hawk.

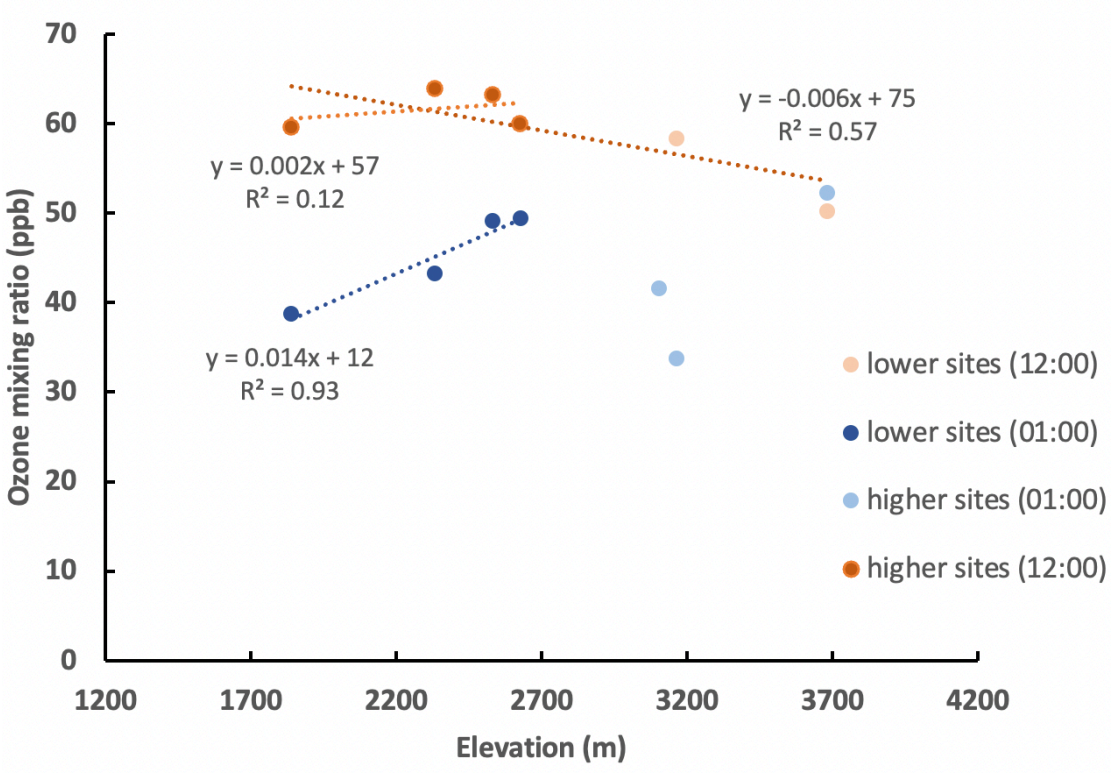

Figure 14. Daytime and nighttime average ozone gradient with elevation. The lower sites (from left to right) are NREL, Vernon, Centennial, and Black Hawk. The higher sites (from left to right) are Jim Creek, St. Mary, and Mines Peak.

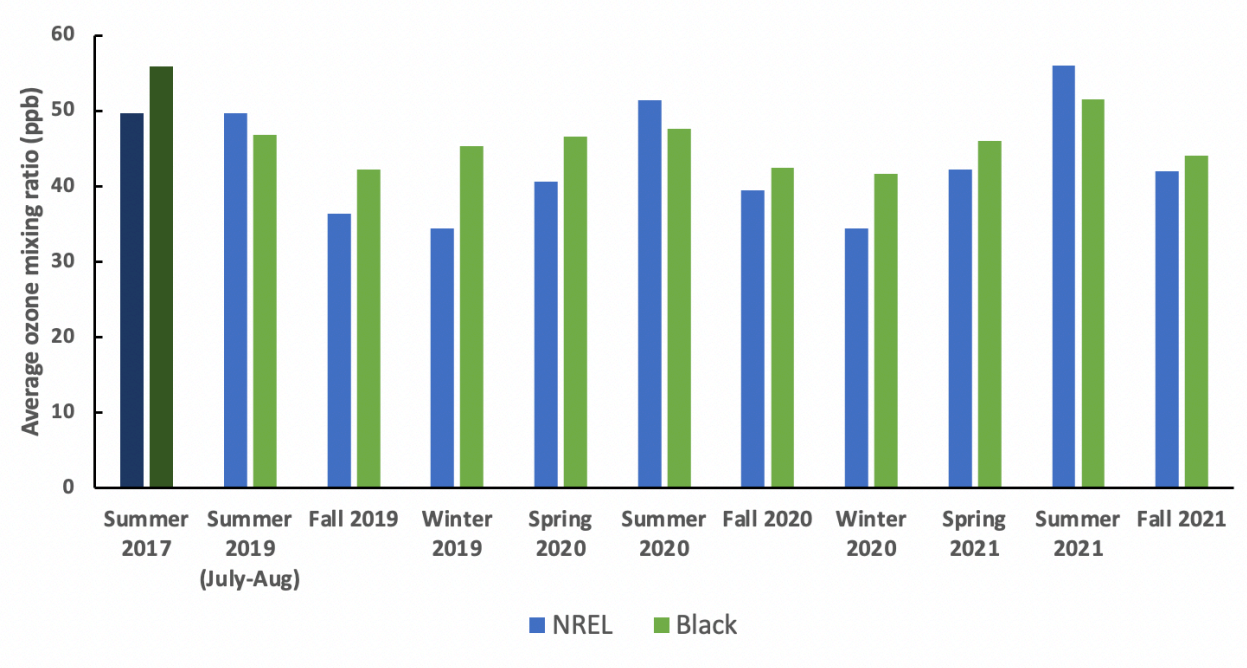

Figure 15. Seasonal average hourly ozone mixing ratios at NREL and Black Hawk from Summer 2017 through Fall 2021. June to August is regarded as summer, September to November is regarded as fall, December to February is regarded as Winter, and March to May is regarded as Spring. The darker colored bars represent the average ozone mixing ratios at these two sites in the 2017 special study period.

9/1/2017

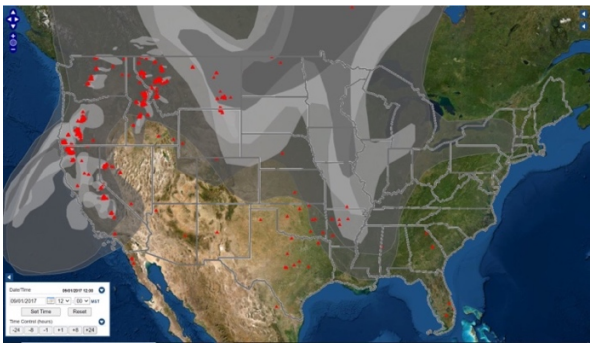

9/2/2017

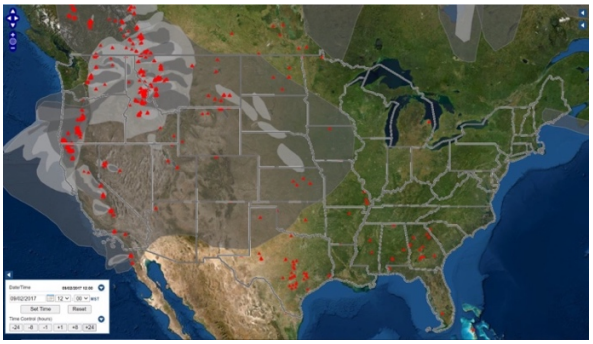

9/3/2017

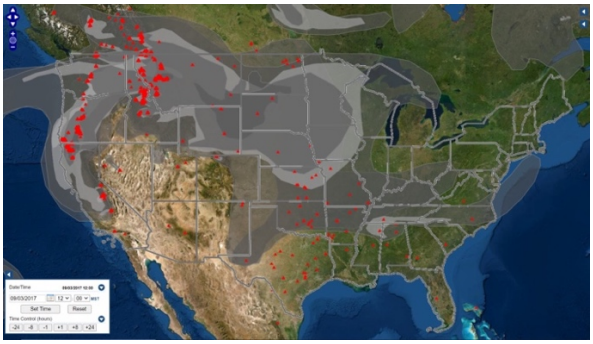

9/4/2017

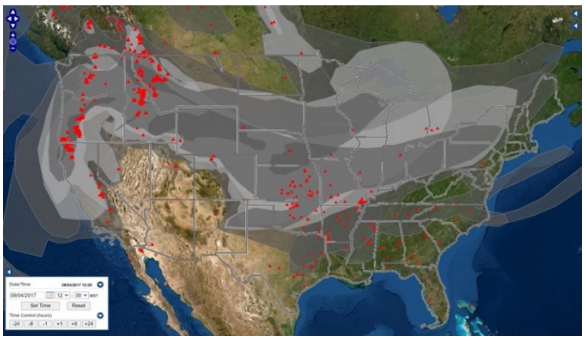

9/5/2017

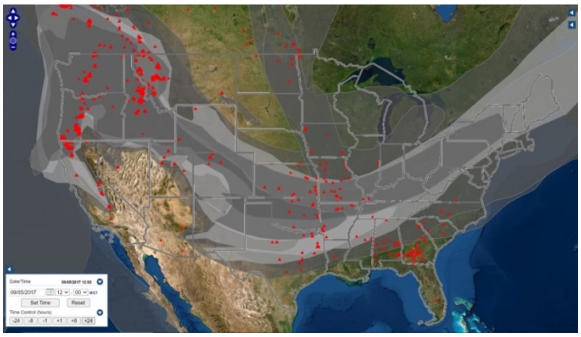

9/6/2017

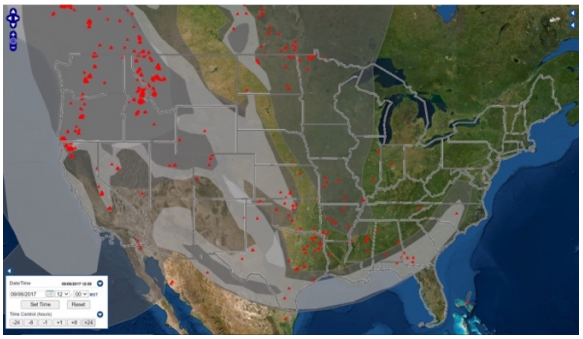

9/7/2017

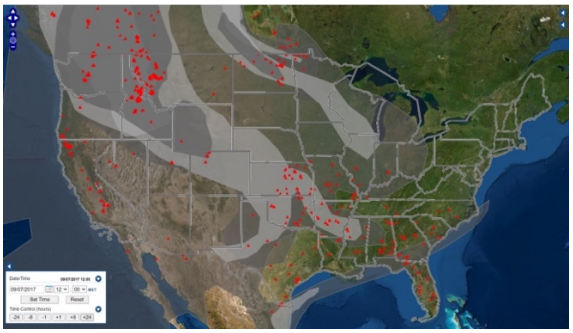

9/8/2017

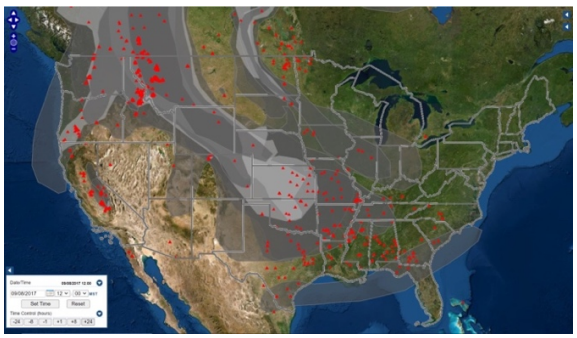

Figure 16. Overhead smoke and fire locations at 12:00 MST every day from September 1st to 8th 2017, retrieved from the HMS Smoke product.

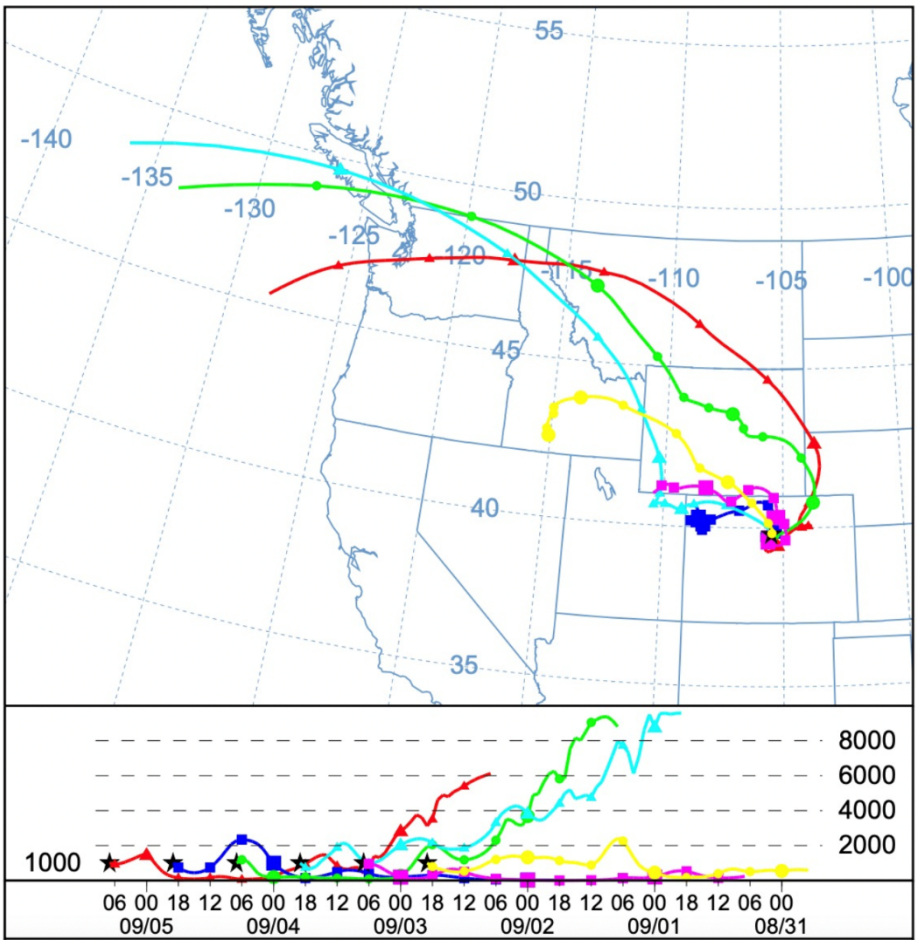

Figure 17. HYSPLIT 72h back trajectories at Black Hawk (39.7928, -105.4973) from 1000m AGL originating September 3 to 5, 2017. The vertical scale of the plot below is in units of meters (AGL).

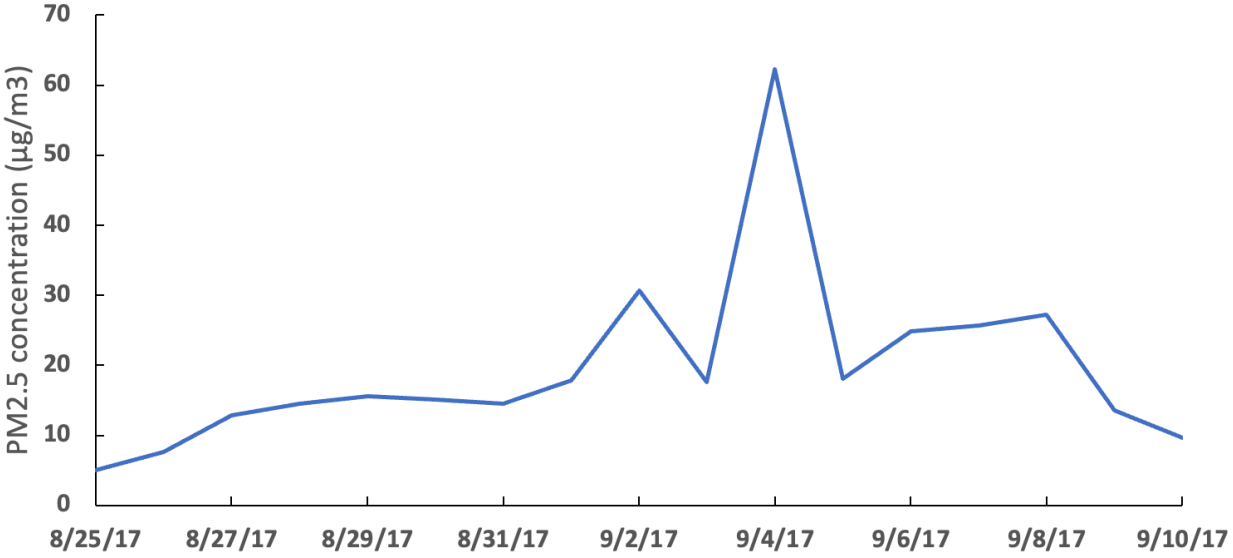

Figure 18. 24-hour mean $PM_{2.5}$ concentration measured at Chatfield Park, the closest PM monitoring site to the transect (25km from NREL), from August 25th to September 10th 2017. The data was obtained from the EPA Air Quality System (AQS) API (https://aqs.epa.gov/aqsweb/documents/data_api.html).

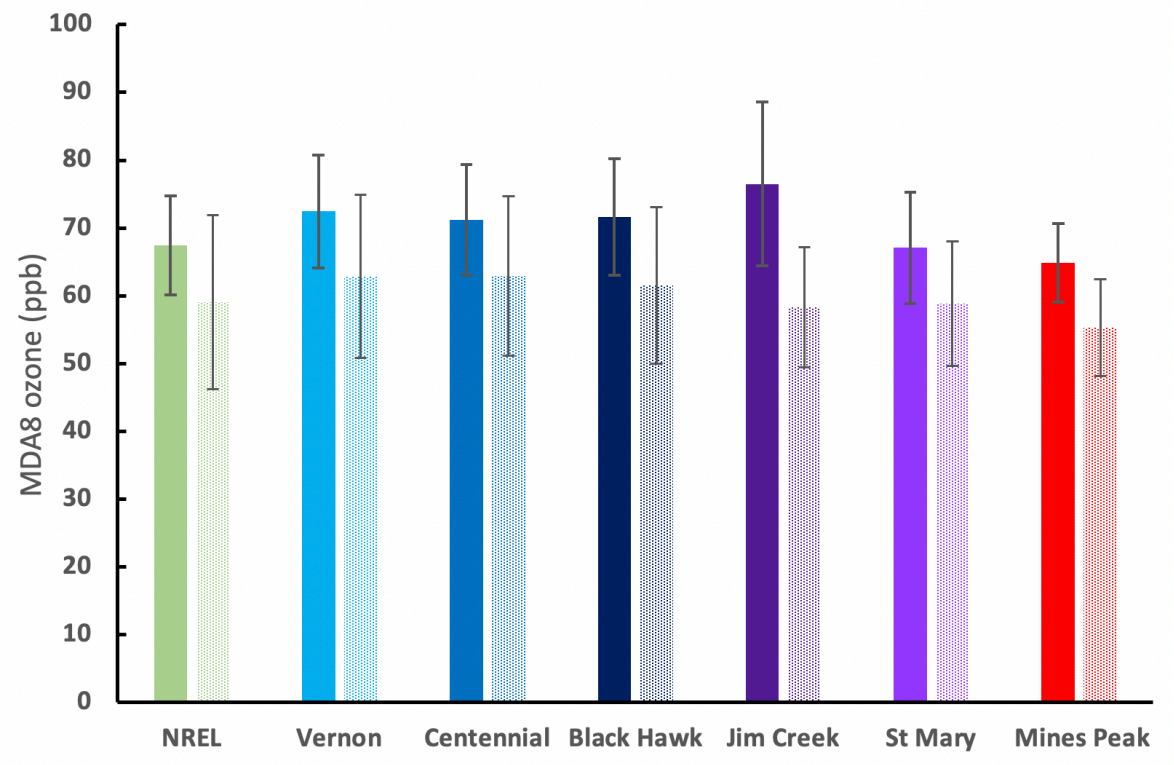

Figure 19. Average MDA8 ozone mixing ratios at all sites from August 27th to September 9th, 2017. The solid bars represent average MDA8 ozone from 8/27 to 9/9/2017, while the dotted bars represent the average MDA8 ozone during non-smoke days (97 days within study period; 25 days of smoke days). The error bars represent standard deviations from average.

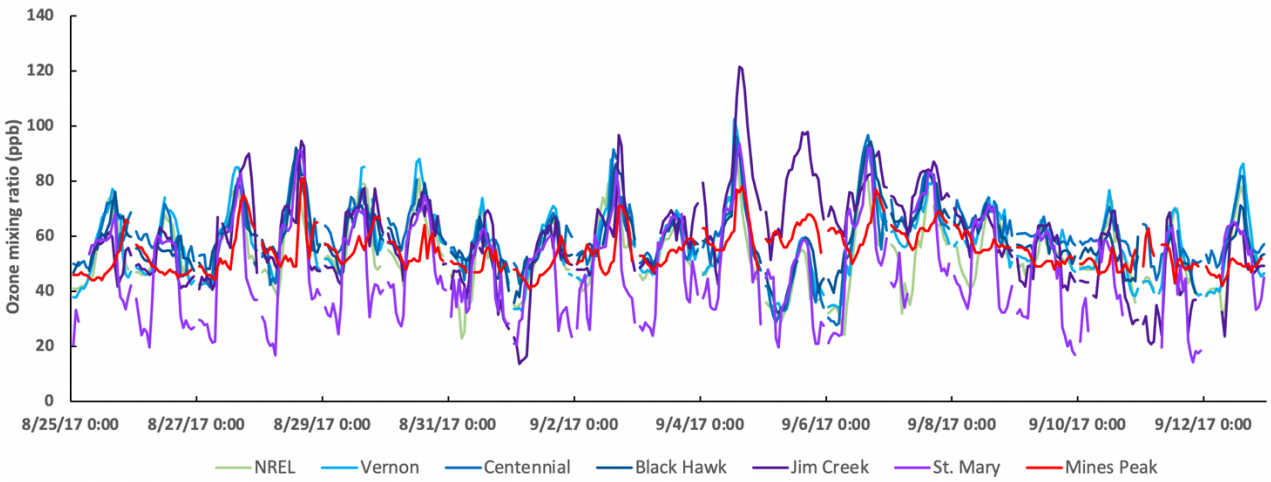

Figure 20. Time series of hourly ozone mixing ratios at all sites from August 25th to September 12th, 2017.

Table 1. Site elevation, location, and description of permanent and temporary sites during the 2017 Denver ozone vertical transect study by CDPHE APCD.

Site Name	**Elevation (m ASL)**	**Latitude**	**Longitude**	**Meteorology**	**Permanent**	**% Data coverage**
NREL	1839	39.7432	-105.1791	No	Yes	70
Vernon	2334	39.7169	-105.2839	Yes	No	91
Centennial	2533	39.7766	-105.3684	Yes	No	92
Black Hawk	2627	39.7928	-105.4973	Yes	Yes (since July 2019)	85
Jim Creek	3104	39.8805	-105.7340	Yes	No	68
St. Mary	3163	39.8091	-105.6398	Yes	No	88
Mines Peak	3683	39.7944	-105.7640	No	Yes	82

Table 2. Descriptive statistics of hourly ozone measurements (in ppb) at all sites along the vertical transect from June 1 to September 30, 2017.

	NREL	Vernon	Centennial	Black Hawk	Jim Creek	St. Mary	Mines Peak
Mean	47	52	54	55	50	47	51
Median	47	52	55	55	49	49	52
Standard Deviation	15	14	13	11	16	17	8
Sample Variance	221	197	180	127	249	274	62
Skewness	0	0	0	0	0	0	0
Range	93	90	84	82	116	93	54
Minimum	8	12	15	16	5	3	27
Maximum	101	102	99	98	122	96	81

Table 3. Average diurnal maxima, minima, and amplitudes (maximum-minimum) of hourly ozone at all sites along the vertical transect.

	NREL	**Vernon**	**Centennial**	**Black Hawk**	**Jim Creek**	**St Mary**	**Mines Peak**
Maximum (ppb)	62	66	65	62	60	59	53
Minimum (ppb)	35	41	45	49	37	32	49
Amplitude (ppb)	26	25	20	13	23	27	4

Table 4. p-values for significance test, R^2, slopes, 95% confidence intervals, and y-axis intercept of linear regressions of the correlations between subsequent day's maximum ozone (10:00 to 16:00) and previous night's average ozone (0:00 to 6:00).

Site	P value	R squared	Slope	Confidence Interval (95%)
NREL	3.1E-05	0.17	0.69	0.38-1.00
Vernon	4.3E-04	0.10	0.54	0.43-0.83
Centennial	3.0E-05	0.14	0.50	0.27-0.73
Black Hawk	0.0095	0.06	0.40	0.10-0.70
St. Mary	1.5E-04	0.11	0.46	0.23-0.70
Jim Creek	2.7E-05	0.20	0.48	0.27-0.69
Mines Peak	2.3E-15	0.43	0.89	0.70-1.1

Table 5. R^2 values of the Pearson pair-wise correlations among all sites' MDA8 values.

	NREL	Vernon	Centennial	Black Hawk	Jim Creek	St. Mary	Mines Peak
NREL	1						
Vernon	0.53	1					
Centennial	0.47	0.91	1				
Black Hawk	0.39	0.74	0.82	1			
Jim Creek	0.21	0.41	0.44	0.50	1		
St. Mary	0.31	0.66	0.69	0.67	0.60	1	
Mines Peak	0.14	0.32	0.36	0.43	0.69	0.57	1